Heat Transport in Glass-Forming Liquids

by

VINAY VAIBHAV
The Institute of Mathematical Sciences
CIT Campus, Taramani, Chennai 600 113, India.

A thesis submitted in partial fulfillment of requirements
for the award of the degree of

Master of Science by Research

of

HOMI BHABHA NATIONAL INSTITUTE

August 2017

Bonafide Certificate

Certified that this dissertation titled **Heat Transport in Glass-Forming Liquids**, is the bonafide work of **Mr. VINAY VAIBHAV** who carried out the project under my supervision.

Signed:
Dr. Pinaki Chaudhuri

Date:

Abstract

We study a model glass-forming liquid under thermal perturbation using the techniques of numerical simulations. The model glass-former that we have used is Kob-Andersen binary Lennard-Jones mixture. We start with a review of different characteristics of supercooled liquids and glasses and then explore some of the equilibrium and non-equilibrium properties of the model glass-former using the techniques of molecular dynamics simulation. We have shown how the age of the system becomes important when it is quenched to the glassy state. We review the techniques of non-equilibrium molecular dynamics and use it to analyze the response of a system to some thermal perturbation. Then we have studied the model glass-former under a non-equilibrium steady situation due to a temperature gradient in z-direction along the length of the system. The temperature gradient is built by thermostating two different regions separated by some distance in the z-direction. We show that a steady heat current has been established in the z-direction. The local number density of all particles in mixture shows unusual behavior for temperatures in the glassy regime.

Acknowledgements

I would like to express my deep gratitude to my thesis advisor Dr. Pinaki Chaudhuri for his continuous guidance and support. I want to thank him for introducing the problem for the thesis and teaching me the required computational skills from scratch.

I would like to thank Ankit Agrawal, SRF in the Computational Biology group at IMSc for helping me out at many occasions.

Contents

List of Figures

Abbreviations

LJ	**L**ennard-**J**ones
MC	**M**onte **C**arlo
MCT	**M**ode **C**oupling **T**heory
MD	**M**olecular **D**ynamics
MSD	**M**ean **S**quared **D**isplacement
NEMD	**N**on-**E**quilibrium **M**olecular **D**ynamics
RDF	**R**adial **D**istribution **F**unction
SCL	**S**upercooled **L**iquid
VFT	**V**ogel **T**ammann **F**ulcher

Symbols

d	Dimension of the system
D	Diffusion coefficient
$\delta(\mathbf{r})$	Dirac delta function
E	Total internal energy of the system
η	Viscosity
f	Number of degrees of freedom
f_{ij}	Force on particle i due to j
$g(r)$	Pair distribution function
i	Particle index
$\mathcal{J}$	Heat current density
j(r,t)	Particle flux
k_B	Boltzmann's constant
L	Box length
m	Mass of the particle
N	Number of particles
P	Pressure
$Q(t)$	Overlap function
r	Particle separation
r	Position of a particle
ρ	Density of the system
t	Time
T	Temperature
T_g	Glass transition temperature

T_m	Melting temperature/Mean temperature
τ	Relaxation time
τ_d	Damping parameter
$\mathbf{v}$	Particle velocity
V	Volume
$V(r)$	Interaction potential
V_{sp}	Specific volume
z	Cartesian coordinate

Chapter 1

Introduction

Liquids or more specifically the glass-forming liquids have been one of the extensively studied systems in last two decades. Disordered materials are much more abundent but many of their properties have not been studied in detail. We still lack a good theoretical model for them. With the increase in the computing power in last some years, it has been possible to probe much deeper in such systems.

This project report studies one of the most popular model glass-forming liquid, Kob-Andersen binary Lennard-Jones mixture [4] [3], under external thermal perturbation. The model glass-former is studied via non-equilibrium molecular dynamics. This work aims at investigating the different parameters of the system with periodic boundary conditions under non-equilibrium steady situation maintained due to a temperature gradient in the system.

The structure of this master thesis is as follows: The whole thesis has been divided into four chapters. Chapter 1 talks about some details of liquids and glass-forming liquids. Chapter 2 presents the details of the tools which have been used to study the system in this report. The main tool which has been used is molecular dynamics. The simulation details under equilibrium and non-equilibrium situation has been discussed in chapter three. Most of the part of this chapter investigates the system via non-equilibrium molecular dynamics at three different temperatures. Conclusions and future directions to this work have been presented in the final chapter.

1.1 Liquids

Most of the systems have liquid as their intermediate phase between solid and gas. Liquids and dense fluids can be distinguished from dilute gases by the way particles collide and the short-range positional correlations while the distinction among liquids and crystals is possible on the basis of long-range order present in periodic lattices. In liquids, the magnitude of total potential energy is comparable to total kinetic energy. Liquids are extensively studied in the computer simulation because unlike solid and gas, no any general simplified and idealized model for liquid exist that could be solved analytically. Liquids have been the most preferred choice for researchers since the beginning of the era of computer simulations.

1.1.1 Model Potentials

Particles of the liquid feel forces due to other particles. The interactions in the liquids are modeled in terms of potentials. The force $\mathbf{F}(\mathbf{r})$ can then be obtained from the corresponding potential $V(\mathbf{r})$ using $\mathbf{F}(\mathbf{r}) = -\nabla V(\mathbf{r})$ [1]. If we consider the interaction among the particles to be pairwise [2] then for small separations it is repulsive while for large separations it is found to be attractive. Hence most modeling potentials have both repulsive and attractive parts. The short range repulsive part is much more crucial because it decides how the particles hard cores pack together which in turn decides the structural properties of the liquid (chapter 1 and 5 of [6]). The attractive forces acting at the longer range have a little contribution in determining the structure of the liquid and are responsible for the cohesive energy which is essential for the stabilization of the liquid. There are various modeling potentials, for example, Hard Sphere, Square-well, Yukawa, Lennard-Jones, WCA etc, which are used depending on the nature of the system. In our simulations, we have considered Lennard-Jones potential as the modeling potential.

[1] although this is possible only if force is conservative

[2] The calculation of any quantity depending on triplets of liquid particles or even higher than this, is time consuming. It is possible to consider an effective pair potential where average three-body effects can be partially included [5]

Lennard-Jones Potential Quantum-mechanical calculations show that at large separations the dominant contribution to the potential comes from multipolar moments induced in one atom due to spontaneous fluctuations in the electronic charge distribution of another atom. The leading term in the multipole expansion varies as r^{-6} which is dipole-dipole interaction (van-der-Waals interaction).

Although the rigorous calculation of short-range interaction creates some technical difficulty [6], but in some approximation, it can be represented by an exponential function of the form $exp(1/r)$. In most cases due to computational and mathematical advantages, the short-range repulsion is usually represented by an inverse power law r^{-n}. Since interaction for larger separations is of the form r^{-6}, therefore, $n = 12$ is the most widely used choice. Lennard-Jones potential incorporating the long range and short range interactions as discussed above has the following form:

$$V(r) = 4\epsilon\left[\left(\frac{\sigma}{r}\right)^{12} - \left(\frac{\sigma}{r}\right)^{6}\right] \tag{1.1}$$

Here the parameter σ is the separation of the particles where $V(r) = 0$ and ϵ is the depth of the potential well at the minimum in $V(r)$. The values of the parameters for different systems can be obtained by studying the atomic collisions [7]. This model of potential has been highly successful in studying rare gas atoms.

1.1.2 Some Important Equilibrium Properties

One often characterize an equilibrium system by some quantities with which it is possible to distinguish it from other systems. These quantities can be either static or dynamic. In thermodynamic limit, when fluctuations go to zero, temperature and energy of the system do not change with time. In such situation, the measurement of static quantities which give structural information can be compared to experiments and simulations. But there are some quantities when they are looked at short time scales, where fluctuations are important then the structure of the liquid changes. Investigation of such quantities becomes important for some systems where the dynamics is very slow and hence structure is changing at much slower rate. An important example of such system is *glass*

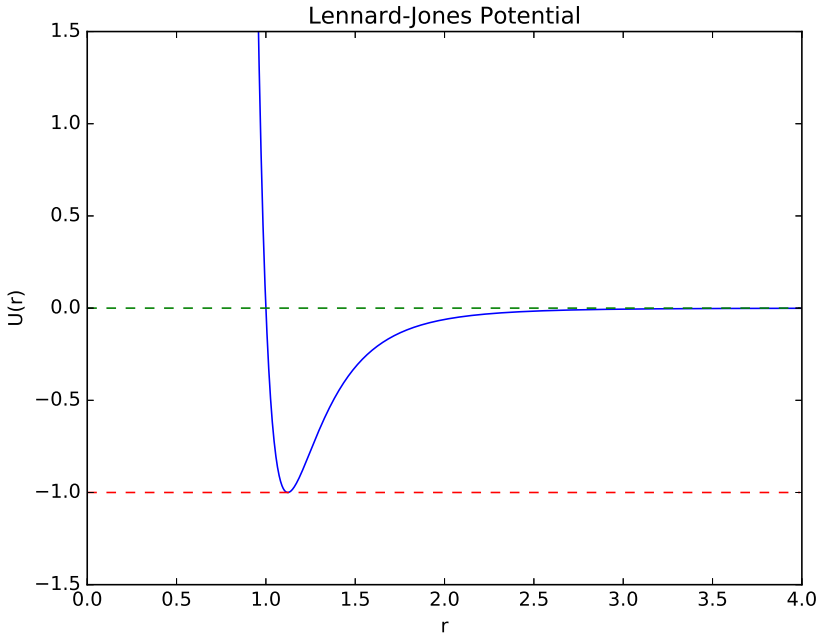

FIGURE 1.1: Lennard-Jones interaction potential with $\sigma = \epsilon = 1$

which looks identical to fluid from the structural point of view but the particles explore their environment on time scales larger than fluids.

Radial Distribution Function Radial distribution function $g(r)$ is one of the important properties that characterize the local structure of a fluid. It is of interest because numerical results of this quantity can be compared with theoretical predictions and also real experiments like neutron and X-ray scattering on simple fluids can produce information about $g(r)$. It is defined as the ratio between the average number density $\rho(r)$ at a distance r from any given atom and the density at a distance r from an atom in an ideal gas at the same overall density. So, $\rho g(r) d\mathbf{r}$ is the conditional probability of finding any other particle in the volume element $d\mathbf{r}$ given that there is a particle at the origin. The general definition of $g(r)$ is given by

$$g(r) = \frac{V}{N^2} \langle \sum_{i=1}^{N} \sum_{j=1, j\neq i}^{N} \delta(r - |\mathbf{r}_j - \mathbf{r}_i|) \rangle \tag{1.2}$$

Radial distribution function is also called two point density correlation function. Computational details of $g(r)$ has seen discussed in section 2.1.2 of chapter 2.

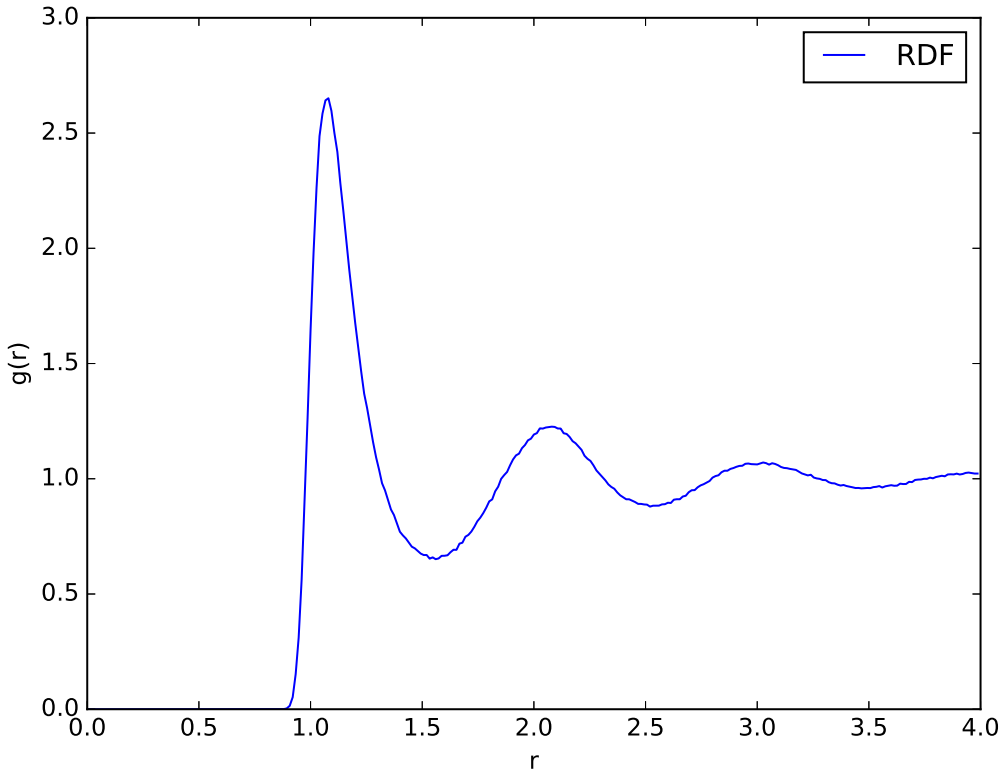

FIGURE 1.2: Radial distribution function of Lennard-Jones fluid with following parameters: N=864, $\rho = 0.8$, T=1.0 and $r_c = 4.0$

This function is constant and equal to 1 for ideal gas while in a crystal $g(r)$ shows sharp peaks due to positional order. For fluids the radial distribution function becomes 1 for large r, meaning that the particle positions are completely uncorrelated while at very short distances, g(r) is zero which is due to the finite particle radius that excludes other particles. For a fluid, a typical radial distribution function looks like Fig. 1.2. The first peak shows the maximum probability of finding another particle and the value of $g(r)$ zero before the first peak is due to the repulsive core of the potential. The minimum followed by the first peak is caused because of exclusion of other particles due to the particles lying in the first shell corresponding to the first peak. Similar to the first peak, all other peaks show particle correlations.

Time Correlation Functions Correlation functions are very useful in determining the dynamic characteristic of a system. If $A(t)$ and $B(t)$ are two dynamic variables of the system, then the time correlation function $C_{AB}(t, t')$ is defined

as

$$C_{AB}(t,t') = \langle A(t+t')B^*(t')\rangle \tag{1.3}$$

where $B^*(t)$ is the complex conjugate of $B(t)$. If the system is in equilibrium, $C_{AB}(t,t')$ becomes stationary, i.e. independent of the time origin t'. These functions are of great interest because their time integrals can be directly related to macroscopic transport coefficients (Green-Kubo relations) [8] [6].

We define here a specific time correlation function called overlap function $Q(t)$, which has been measured in the simulations performed in section 3.2. Pair correlation function represents spatial correlation of densities and hence it gives the information about the structure of the material. But overlap function is a temporal correlations of densities and hence it gives the information about the change in structure of the material or in other words, it measures the overlap of structure at some instant with the structure at some other instant. The overlap function $Q(t)$ is defined as [9],

$$Q(t) = \langle \rho(\vec{r},t_o)\rho(\vec{r},t+t_o)\rangle = \int d\vec{r}\rho(\vec{r},t_o)\rho(\vec{r},t+t_o) \tag{1.4}$$

where $\rho(\vec{r},t_o)$ is space time dependent particle number density. This expression for $Q(t)$ can be approximated with [9],

$$Q(t) \sim \sum_{\iota=1}^{N} w(|\vec{r}_i(t_o) - \vec{r}_i(t_o+t)|) \tag{1.5}$$

where $w(r)$ is called window function, $w(r) = 1$ if $r \leq a$ and zero otherwise. The value of a depends on the system under consideration. If the structural changes in the system is fast then $Q(t)$ decreases sharply with time but for the system where dynamics is slow (for e.g. glass), $Q(t)$ shows very slow decrease.

Mean Squared Displacement and Diffusion At very short times, the behaviour of mean squared displacement ($\langle \delta\mathbf{r}^2(t)\rangle$) is proportional to t^2, which corresponds to free-particle (or 'ballistic') motion [6]. This is identical with the motion of ideal gas. The long time behaviour of mean squared displacement (MSD) is proportional to t which can also be related to diffusion coefficient as discussed below. Diffusion is caused by the molecular motion of fluid particles. Diffusion of a labeled species among identical type of species is called self-diffusion.

Fick's law states that a concentration gradient results in a particles flux $\mathbf{j}(\mathbf{r},t)$ against this density gradient - for slow and small density fluctuations this relation becomes linear:

$$\mathbf{j}(\mathbf{r},t) = -D\nabla\rho(\mathbf{r},t), \tag{1.6}$$

where D is referred as diffusion coefficient and $\rho(\mathbf{r},t)$ is the density of diffusing particles in position $\mathbf{r}$ at time t. Conservation of particles number leads to continuity equation,

$$\frac{\partial}{\partial t}\rho(\mathbf{r},t) + \nabla\cdot\mathbf{j}(\mathbf{r},t) = 0 \tag{1.7}$$

Conservation equation combined with Fick's law gives diffusion equation:

$$\frac{\partial}{\partial t}\rho(\mathbf{r},t) = D\nabla^2\rho(\mathbf{r},t) \tag{1.8}$$

This equation can be solved by defining the Fourier transform of $\rho(\mathbf{r},t)$ with boundary condition $\rho(\mathbf{r},t) = \delta(r)$ ($\delta(r)$ is Dirac delta function). The solution for $\rho(\mathbf{q},t)$ can be written as,

$$\rho(\mathbf{r},t) = \frac{1}{(4\pi Dt)^{d/2}} exp(-\frac{r^2}{4Dt}) \tag{1.9}$$

where d is the dimensionality of the system. Assuming $\int d\mathbf{r}\rho(\mathbf{r},t) = 1$, the second moment of $\rho(\mathbf{r},t)$ can be written as:

$$\langle r^2(t)\rangle = \int d\mathbf{r}\rho(\mathbf{r},t)r^2. \tag{1.10}$$

Multiplying equation 1.8 with r^2 and integrating over all space gives the time evolution of $\langle r^2(t)\rangle$. With some simplification we can write,

$$\frac{\partial\langle r^2(t)\rangle}{\partial t} = 2dD \tag{1.11}$$

This equation called Einstein relation, relates diffusion constant D to the width of the concentration profile. $\langle r^2(t)\rangle$ is a microscopic parameter which is in fact the mean-squared distance over which the labeled particle has moved while D is a macroscopic transport coefficient. This also provides the way to measure D in computer simulations.

1.2 Supercooled Liquids and Glasses

In normal situation when a liquid is cooled then it may undergo a first order phase transition resulting in crystal[3]. This can be identified with a sharp change in specific volume (see Fig.1.3) at a temperature T_m, the melting point. But sometimes what happens that a liquid manages to be in the liquid state even below T_m without crystallizing. Such liquid is called supercooled liquid (SCL). The chance of a liquid to be in the supercooled state rather than crystallizing during cooling depends upon cooling rate, the presence of impurity in the liquid, the composition of the liquid (if mixture), the viscosity at T_m and many other factors. As a supercooled liquid is cooled to lower temperatures, its viscosity in-

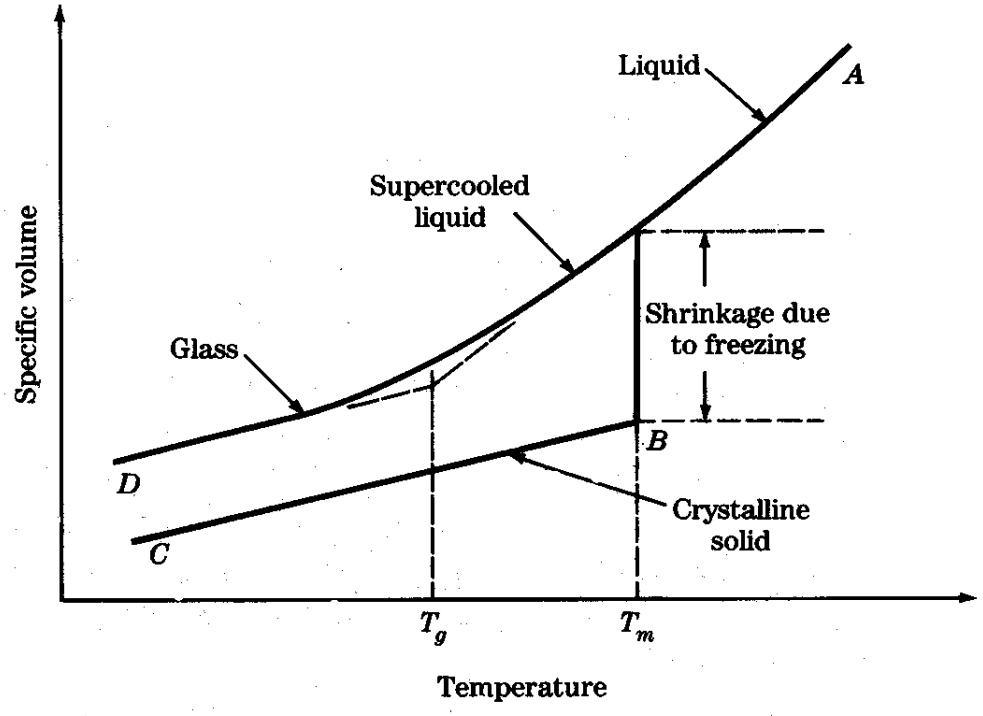

FIGURE 1.3: Schematic representation of the specific volume as a function of temperature for a liquid which can both crystallize and form a glass (https://www.benbest.com/cryonics/cooling.html).

creases and the molecular motion becomes slower. At some temperature (called glass transition temperature T_g) the molecules will be moving so slowly that they do not have a chance to rearrange significantly before the temperature is lowered further. As a result, the experimentally observed specific volume begin to deviate from the expected equilibrium value. If the temperature is further lowered by a very small amount, time scales for molecular rearrangements become

[3]This whole section is mainly based on following references: [10] [1] [11]

surprisingly long, compared to the time scale of the experimental observation. The structure of this material is almost frozen for all practical purposes and the system in this state is called glass. The glass transition temperature T_g can be defined by extrapolating V_{sp} in the glassy state back to the supercooled liquid line (Fig. 1.3). The system below the glass transition temperature runs out of equilibrium and it keeps on relaxing. Hence in such situation, if any property associated with the system measured, it depends on the point of time when the measurement is made. This phenomenon is called aging [12].

Dynamics Near Glass Transition Temperature Supercooled liquids have very high viscosity near T_g hence, the flow becomes very slow and behaves as solid for many purposes. Also, the time scale for molecular motions increases dramatically. The three liquids shown in the Fig. 1.4 have different temperature dependencies as T_g is approached. Sometimes glass transition temperature is

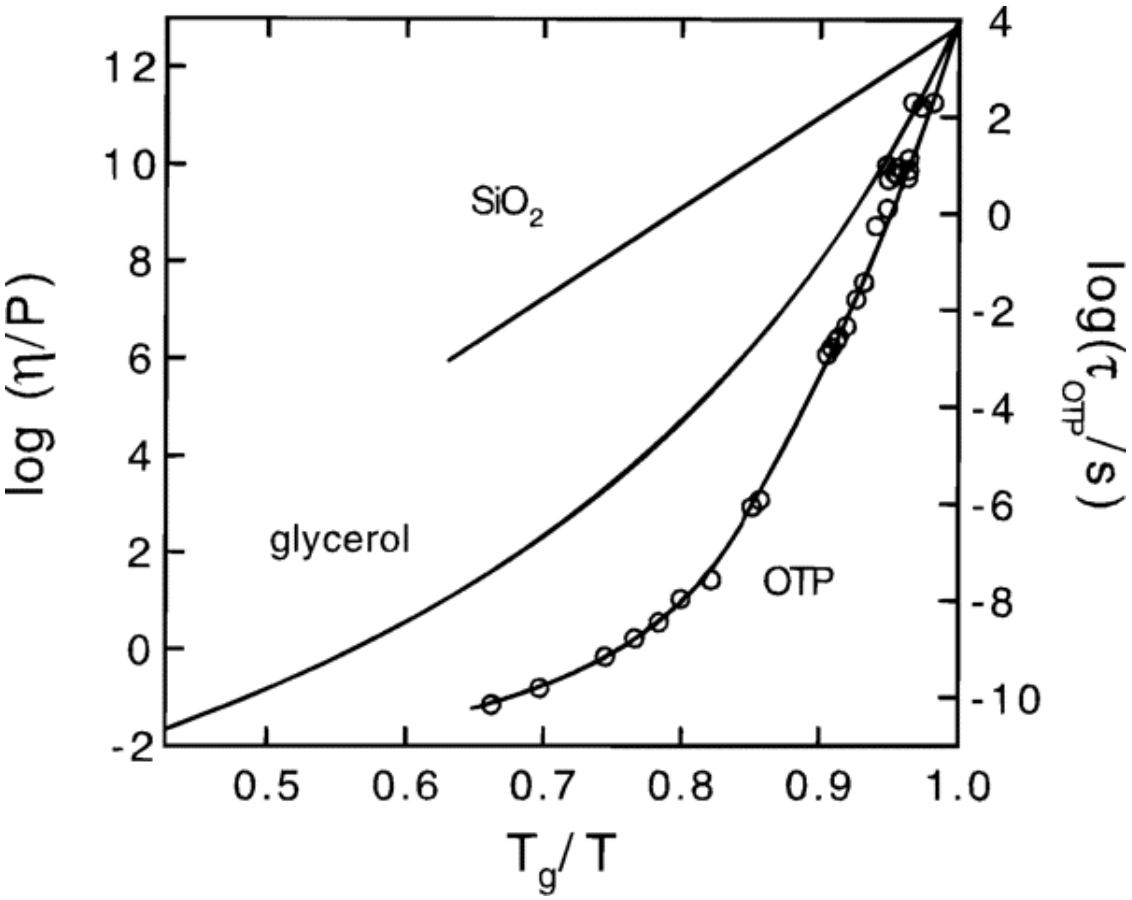

FIGURE 1.4: Dependence of viscosity η on temperature for three three liquids: SiO_2, glycerol and o-terphenyl. SiO_2 shows the characteristic of strong liquid while the other two liquids are fragile. Relaxation time dependence on temperature has been shown only for o-terphenyl (O) [1].

defined in terms of the viscosity of the SCL: T_g is the temperature at which the viscosity of the liquid near $10^{13}P$. Depending on the nature of relaxation, supercooled liquids can be either strong or fragile. Strong liquids (for e.g., SiO_2) are characterized by Arrhenius relaxation [4] processes while fragile liquids have quite non-Arrhenius relaxation behavior. Temperature dependence of relaxation times (or the viscosity) for supercooled liquids is often described at least approximately by the Vogel-Tammann-Fulcher (VTF) equation:

$$\tau = \tau_o exp\left(\frac{B}{T - T_\infty}\right) \tag{1.12}$$

where τ_o, B and T_∞ are constants. For $T_\infty > 0$, the temperature dependence of relaxation time is non-Arrhenius and at $T = T_\infty$ called Vogel-temperature, the relaxation time is predicted to be infinite.

VFT law is completely phenomenological. There exist only few theories capable of describing the relaxation process to a good extent. Mode coupling theory (MCT) is one of them. In order to describe the increasing viscosity and relaxation timescales, MCT predicts that relaxation time τ or viscosity η diverges as a power law:

$$\tau \propto \frac{1}{[T - T_{MCT}]^{-\gamma}} \tag{1.13}$$

Here T_{MCT} is a critical temperature called mode coupling temperature and γ is an exponent whose value depends on the glass-former. It is believed that the equilibrium properties of the glass-former are satisfactorily described by MCT. But many people believe that near glass transition temperature T_g, MCT is not the ultimate theory.

In this report, we study the thermal response of a fragile glass-former. So, let's discuss the thermal properties and the problem of heat transport that we want to address, in glassy systems.

1.3 Heat Transport in Glasses

The thermal properties of disordered materials like glasses can be far more interesting than crystalline solids. Due to periodicity in crystalline solids, the study of

[4] the relaxation of the form exp(-E/k_BT), where E is activation barrier

their thermal properties becomes easy and they have been studied in sufficient detail but in contrast, the thermal properties of disordered materials like glass are poorly known and need to be explored. Detailed knowledge of thermal properties of glassy materials can have many commercial and technical advantages. Generally, glasses are believed to be bad conductor of heat and their conductivity can show dependence on temperature. Since the heat conduction happens via microscopic collisions of atoms and the atoms in glassy state are almost trapped, hence the study of thermal properties of glasses can have wide consequences.

In this report, we try to explore the thermal transport properties of a well-known model glass-former (Kob-Andersen binary Lennard-Jones mixture) in the supercooled regime and also in the glassy regime. The system is studied under a thermal perturbation, using the techniques of non-equilibrium molecular dynamics (NEMD).

Chapter 2

Tools and Techniques

Computer simulations provide a means to explore the properties of a physical system using some mathematical description or by modeling appropriately the real system. Broadly, the computer simulation methods in statistical mechanics can be categorized as Monte Carlo (MC) and Molecular Dynamics (MD). In both methods, the thermodynamic averages of measurable quantities are determined by evolving the model system through a set of microstates. Computer simulations have been successful in studying not only the equilibrium systems but also non-equilibrium processes. MC uses pseudorandom numbers to generate a representative configuration of the system while in MD simulations Newton's equations of motion are solved to determine the configuration of the system. So in this respect, it can be said that MC is probabilistic or stochastic but MD (when it samples from NVE ensemble) is deterministic.

MC and MD simulations both investigate the macroscopic properties of atomic or molecular systems. These techniques are applicable to a variety of systems ranging from a simple monoatomic fluid to complex multiatomic protein. Real systems always have very large number of degrees of freedom. One can have the feel of the size of the system by looking at the fact that even one mole of a substance correspond to the number of particles of the order of 10^{23}. Since computers have the limited capacity of handling up to few million degrees of freedom, so it becomes necessary to reduce the size of the system so that it could be conveniently handled in computers. Hence one has to use some techniques to make sure that the results obtained represent the behavior of systems in the thermodynamic limit.

Whether to determine the average properties of a system, MD or MC should be used, depends on the type of the system. Both techniques have their own limitations. MD can be used to study only classical systems and it explores then region close to initial configuration only. On the other hand, MC can be used for both classical and quantum systems and capable of covering the most of the portion of phase space. But since in MC there is no any time dimension hence dynamical quantities cannot be calculated but MD can calculate them. As here we need to calculate many dynamical quantities hence we shall use MD to study the properties of the system. This chapter presents the technique of equilibrium and non-equilibrium MD in detail.

2.1 Introduction to Molecular Dynamics Simulation

The technique of molecular dynamics is widely used to calculate the equilibrium and transport properties of a classical N-body system. For an N-body system, we 3N set of equations of motion. MD provides a systematic way to solve these equations at regular interval of time which gives the time evolution of the system. The Born-Oppenheimer approximation guarantees the validity of the use of classical equations of motion to study atomic or molecular systems. The very first molecular dynamics study of Lennard-Jones fluid was done by Rahman in 1964 [13]. In this report, we will always consider atomic system. This section talks about equilibrium molecular dynamics while the next section explains the technique of non-equilibrium molecular dynamics.

2.1.1 Structure of a Generic Molecular Dynamics Program

The construction of a simple Molecular Dynamics Program involves following steps:

- Setting up the details of the initial conditions of the system. These initial conditions can be the number of particles, density, initial temperature etc.
- Initializing the positions and velocities.
- Computing the force acting on all particles according to the interacting potential between particles.

- Using some integrating algorithm, finding the next configuration of the system after a small time interval δt. This step and the previous one can be repeated until the required length of evolution is achieved.
- Computing the averages of the desired physical quantities.

Out of above steps, the important steps are initialization, force calculation and system evolution using integrating algorithms. These steps need little description so let's discuss them in detail.

Initialization Although, in principle, equilibrium properties of a system should not depend on the choice of initial conditions, but one should be careful while choosing this. If somehow the calculation of the properties depend on initial conditions then either the system is behaving nonergodically (this happens in some low-temperature disordered solids including glassy systems) or it has still not reached equilibrium.

At first, a simulation box should be decided with box dimensions based on the specified density of the system and all the particles should be assigned initial positions within the box along with some appropriate initial velocities. The shape of the box can be rectangular, spherical, cylindrical or one of the many other possibilities. Here, throughout our simulation, we have used a rectangular box with fixed boundaries. The best way to assign positions of the particles in the box is to place them over some lattice. Placing particles randomly may result in overlapping or some of them may be so close that there can be very large forces which will make the system unstable. If there is no other option than placing particles randomly (maybe in the case of systems having a mixture of particles) then energy minimization [1] should be performed before proceeding with simulation. We need to be little careful while initializing positions of a system if we are interested in its fluid phase. Most of the time, the system prepared initially on some lattice (which in fact correspond to some solid) will melt subsequently. But in some cases, the structure can be metastable. So, to avoid any such situation, it is better to start with some final configuration of a fully equilibrated liquid system by adjusting its density and temperature.

[1] Energy minimization: It is the process of changing the arrangement of system particles such that the net inter-particle force on each particle is close to zero and the position of the system on potential energy surface is close to a stationary point.

The initial velocities of the particles should be assigned as per the initial temperature of the system. The instantaneous temperature of the system is decided by the average kinetic energy of the system i.e., $\frac{f}{2}k_BT = \langle\text{kinetic energy}\rangle$ where f is the number of degrees of freedom of system (also see section 2.1.2), as per the law of equipartition of energy. Although this initial setting of the velocities based on initial temperature is not important because they will be adjusted during equilibration (see section 2.1.3). So, we can assign velocities with the random numbers chosen from a uniform distribution (say $[-0.5, 0.5]$ [2]). If we really want the initial velocities to correspond the initial temperature of the system then either we can rescale the components of the random velocities chosen from a uniform distribution or we can directly choose them from a Maxwell distribution corresponding to the initial temperature. In whatever way we assign the initial velocities, we should always take care that the different components of momenta of the system are set to zero if the simulation is to be done at constant energy.

Force Calculation Calculation of the force acting on each particle is necessary, in order to evolve the system based on Newton's equations of motion. Assuming, the interaction to be pairwise and additive, we need to consider the contribution from all the other particles in the box, to find the force on a particle. Most of such force calculations involve calculation of interparticle separations. While calculating interparticle separations, boundary conditions should also be applied. The boundary conditions can be either free or hard or periodic. In most situations, if a system is not having long range interaction, periodic boundary conditions (section 2.1.5 talks more about this) are the best choice since it mimics an infinitely sized system.

Finding the Next Configuration Now after calculating the forces acting on particles, we can use Newton's equations of motion to make an evolution of the system. If $\mathbf{F}_i$ is the net force acting on a representative particle i at position $\mathbf{r}_i$ with mass m_i then we can write:

$$m_i \frac{d^2}{dt^2}\mathbf{r}_i = \mathbf{F}_i \tag{2.1}$$

[2] could be $[-1, 1]$ but taking higher value of initial velocities may lead to instability in the system

We have equations like this for each particle in the box, in total 3N equations. There are many algorithms to solve such equations numerically so that we can have positions and velocities of all particles after a small time interval [5]. One of the most widely used algorithms in MD is *Verlet integration* scheme. This algorithm is not only time reversible but also symplectic (means it preserves the phase space volume).

Its derivation is based on the Taylor expansion of position of a particle $\mathbf{r}(t)$. If δt is the time step length of simulaion then

$$\mathbf{r}(t+\delta t) = \mathbf{r}(t) + \dot{\mathbf{r}}(t)\delta t + \ddot{\mathbf{r}}(t)\frac{\delta t^2}{2} + \dddot{\mathbf{r}}(t)\frac{\delta t^3}{6} + \mathcal{O}(\delta t^4) \tag{2.2a}$$

$$\mathbf{r}(t-\delta t) = \mathbf{r}(t) - \dot{\mathbf{r}}(t)\delta t + \ddot{\mathbf{r}}(t)\frac{\delta t^2}{2} - \dddot{\mathbf{r}}(t)\frac{\delta t^3}{6} + \mathcal{O}(\delta t^4) \tag{2.2b}$$

Adding the equations in 2.2 gives,

$$\mathbf{r}(t+\delta t) = \mathbf{r}(t-\delta t) + 2\mathbf{r}(t) + \ddot{\mathbf{r}}(t)\delta t^2 + \mathcal{O}(\delta t^4) \tag{2.3}$$

Using equation 2.1 in last equation gives the position of a paricle at $t+\delta t$, correct to the order δt^4, in terms of its positions at t and $t-\delta t$ and the force acting on it at t.

$$\mathbf{r}(t+\delta t) \approx \mathbf{r}(t-\delta t) + 2\mathbf{r}(t) + \frac{\mathbf{F}(t)}{2m}\delta t^2 \tag{2.4}$$

Clearly, the computation of new positions is independent of the velocities. But once positions are calculated then using them, velocities can also be calculated. Because if we subtract equations in 2.2 then we get velocity of a particle at t, correct to the order δt^2, in terms of its positions at $t+\delta t$ and $t-\delta t$.

$$\mathbf{v}(t) \approx \frac{1}{2\delta t}[\mathbf{r}(t+\delta t) - \mathbf{r}(t-\delta t)] \tag{2.5}$$

Here from equations 2.4 and 2.5, it is clear that positions and velocities both cannot be determined at same time. Since, velocities are used in computation of kinetic energy, so potential and kinetic energy both cannot be determined at same time which make computation of total energy difficult. However, it is possible to put Verlet algorithm in slightly different form called *velocity Verlet* algorithm [14] , where computation of positions and velocities is possible at same time:

$$\mathbf{r}(t+\delta t) = \mathbf{r}(t) + \mathbf{v}(t)\delta t + \frac{\mathbf{F}(t)}{2m}\delta t^2, \tag{2.6}$$

$$\mathbf{v}(t+\delta t) = \mathbf{v}(t) + \frac{\delta t}{2m}[\mathbf{F}(t+\delta t) + \mathbf{F}(t)] \tag{2.7}$$

In this scheme, computation of positions at $t + \delta t$ requires the knowledge of positions, velocities and forces at t. These new positions should be used to compute forces at $t + \delta t$, because which are essential for the computation of velocities at $t + \delta t$. As, this algorithm is derived from Verlet algorithm so, it generates indentical trajectories.

Every time after generating new postions, we make sure the particles crossing the box boundaries enter the box again from opposite side so that periodic boundary conditions are always maintained. Then using the newly generated positions and velocities, different thermodynamic quantities like kinetic energy, potential energy etc (see section 2.1.2 for the details of computation of diffrent thermodynamic quantities) can be calculated.

2.1.2 Measuring Properties

Now we discuss, once a working MD program is ready, how can it be used to measure the different macroscopic properties of the system. It is necessary to remember that in MD program we can generate the configurations (positions and velocities of particles in the system) of the system at some interval of time δt. So, whatever properties we measure, has to be expressed in terms of average of some function of the coordinates and velocities except for some quantities like entropy, free energy etc which cannot be expressed in terms of such function [3].

The properties can be either measured runtime on the fly or by analyzing the configuration files saved at an interval of few time steps. Most of the properties which depend on interparticle separations like potential energy, pressure, are measured runtime because the calculation of interparticle separations is the most time consuming part of any MD program. Now let's discuss the details of the measurement of some important properties in MD simulations.

Temperature: As mentioned earlier, the temperature can be measured by computing the average kinetic energy per degree of freedom. If f is the number of degrees of freedom of the system then the instantaneous temperature T of the

[3] for measuring such quantities some special techniques are needed (see Chapter 7 of [2] or [5])

system can be given by

$$T = \frac{2}{f}\langle \text{kinetic energy} \rangle \tag{2.8}$$

For a simple $3D$ atomic system with N particles [4],

$$T = \frac{2}{3N-3}\sum_{i=1}^{N}\frac{1}{2}m_i\mathbf{v}_i^2 \; = \frac{1}{3N-3}\sum_{i=1}^{N}m_i\mathbf{v}_i^2$$

where **v** is the velocity of ith particle with mass m_i.

Pressure: Generally pressure is calculated using the virial equation of state [15]:

$$P = \rho T + \frac{1}{dV}\left\langle \sum_{i<j}\mathbf{F}(\mathbf{r}_{ij})\cdot\mathbf{r}_{ij} \right\rangle \tag{2.9}$$

where ρ is the density of system in d dimension and $\mathbf{F}(\mathbf{r}_{ij})$ is the force between particles i and j separated by $|\mathbf{r}_{ij}|$[5].

Radial Distribution Function: Section 1.1.2 has discussed the RDF in detail. Here we discuss the details of computation of RDF. A very comprehensible algorithm to compute RDF has been discussed in Algorithm-7 of chapter 4 of [2]. Let's talk about that algorithm in brief.

Generally, RDF is computed by analyzing the few configurations saved during the simulation or it can be computed runtime. At first, a length equal to half of the box (or some other fraction of box length depending on the cutoff of potential) is divided into many bins and a counter in each bin is set to zero. Then with respect to each particle the separation of other particles, lying within interaction range, is calculated and for each such separation, the counter in the corresponding bin is increased by 1. Now assuming the box filled with ideal gas, the number of particles corresponding to one bin is calculated (in this case of ideal gas each bin will correspond to the same number of particles) and each bin (of the real system) is divided by this number. Finally, the plot of this normalized number in each bin along the half length of the box gives radial distribution function.

[4] for N-particle atomic system the number of independent degrees of freedom is $3N-3$ because due to fixed zero momentum, center of mass is at rest

[5] this expression for pressure is strictly valid for the system at constant temperature but people loosely use it for the system at constant energy

2.1.3 Equilibration

While performing equilibrium simulations, before one starts collecting the data it is necessary to make sure that the system has reached the equilibrium state that we want. Most of the time the initial configuration of the simulation is at some different temperature or density then it becomes necessary to run the system for some period such that it reaches the required equilibrium state. This initial period of the run is called equilibration. After equilibration, no memory of initial configuration is left. In normal cases equilibration is confirmed by monitoring the potential energy and pressure. Equilibration is continued until these quantities start to fluctuate about some mean value. Sometimes for simulating liquid phase (also see here 2.1.1) the starting configuration is taken over some lattice then such systems need equilibration. In such cases some structural quantities like translational or rotational order parameter, radial distribution function, structure factor etc (see page 171 of [5] for details) can be monitored which confirm melting of lattice and progress to equilibration. It is also useful to monitor the mean squared displacement (MSD) of particles from their starting positions. Equilibration can be confirmed if this function starts showing a linear dependence on time. Because MSD increases if the system is in the liquid phase and oscillates around a mean value for simulation in the solid phase. Monitoring this quantity can be helpful for the simulations which starting configuration is not only a lattice but a disordered configuration where there is a chance that the system may be trapped in a glassy state.

One of the characteristics of an equilibrated system is, if the system is set free at constant energy then the temperature of the system does not show any systematic drift. Also, if one needs an equilibrated system at some particular temperature then the temperature of the system should be set via thermostating during equilibration.

2.1.4 Thermostating

In real experiments whenever we need to maintain the temperature of a system, it is brought in contact with some reservoir at the desired temperature. In simulations, there are various techniques which are used to maintain the temperature of the system. Sometimes the aim of thermostating is just to take the system to

some particular temperature and run the simulation at constant energy. In such cases, the way of thermostating is not much important. Because after equilibration, the system forgets the history. But if one has to do the simulation at constant temperature then the choice of thermostat matters. Because here we require the generated trajectories to correspond to a true canonical ensemble. Some of these techniques have been discussed below.

Velocity Scaling: This is the simplest way of thermostating. If $T(t)$ is the current temperature of the system and T_0 is the desired temperature that one wants to maintain then in velocity scaling, the velocity of each particle is multiplied by a factor $\lambda = \sqrt{T_0/T(t)}$ after each time step or at an interval of few time steps. This process is repeated up to some time steps depending on the nature of the system. When rescaling is used then system jumps from one point to another point in phase space which is completely unphysical, that's why this thermostat is not frequent in use.

Berendsen Thermostat: This is the weaker formulation of scaling. In this method, the system is coupled to an external heat bath at the desired temperature T_0 and the velocities are scaled at each step, such that the rate of change of temperature is proportional to the difference in temperature:

$$\frac{dT(t)}{dt} = \frac{1}{\tau}(T_0 - T(t)) \tag{2.10}$$

where τ is the coupling parameter which determines how tightly the bath and the system are coupled together. The temperature of the system reaches the desired temperature exponentially. For the very low value of τ, the thermostating is violent and fluctuations in temperature become so small that it become unrealistic. Moreover, the very large value of τ makes the thermostat inactive. Similar to scaling, this thermostat also doesn't generate a true canonical ensemble.

Andersen Thermostat: This method of thermostating, suggested by Andersen [16], is one of the simplest methods which correctly samples the NVT ensemble. Andersen thermostat is based on the way in which a real system is thermostated when brought in contact with a heat bath. In a real system, a fraction of molecules keep colliding with the bath and hence exchange of energy continuously takes place which in turn maintain the temperature of the system. Here also in Andersen thermostat, at each step, some prescribed number of particles are selected and their velocities are replaced with the velocities drawn from a

Gaussian distribution at the prescribed temperature. The selection of particles mimic the particles which undergo a stochastic collision with the bath in a real system. The strength of coupling to the heat bath is determined by the frequency ν of stochastic collisions. In simulation, for each particle a random number is generated between 0 and 1, if this number is less than $\nu\Delta t$ then particle velocities are replaced [2].

Langevin Thermostat: In Langevin thermostat at each time step, all particles receive a random force and a frictional force which correspond to the case of Brownian motion following Langevin equation of motion. In this method the particle's equation of motion is modified via the following equation:

$$m\ddot{\mathbf{r}}_i = -\nabla_i V(r) - m\gamma\dot{\mathbf{r}}_i + \mathbf{W}_i \tag{2.11}$$

where γ is the friction coefficient (damping parameter) and $\mathbf{W}_i$ is the random force acting on the ith particle. The average magnitude of the random forces and the friction are related in such a way that fluctuation-dissipation theorem is obeyed, which guarantees NVT statistics. To implement this thermostat a subroutine which calculates the forces acting on each particle is modified such that the randomly generated forces are added to the calculated forces and the integrator is modified to incorporate the effects of damping.

Andersen thermostat and Langevin thermostat are based on stochastic processes and both thermostats are capable of generating a canonical ensemble. But there is an another technique where the temperature is maintained by deterministic Molecular Dynamics at a constant temperature. One such thermostat is Nose-Hoover Thermostat. Here the idea of extended-Lagrangian is used where some extra degrees of freedom are introduced into the Lagrangian for the N-body system [2]

2.1.5 Periodic Boundary Conditions

As discussed previously, there is a limitation on the size of the system that can be handled conveniently in computers. For smaller systems an appreciable fraction of particles lie near the boundary and hence for such systems the choice of boundary conditions, whether it is free or hard or periodic, can have severe

effects. Often we are interested in the properties of the system in the thermodynamic limit. By considering periodic boundary conditions it is possible to mimic a pseudo-infinite system where a particle leaving the simulation box enters the box again from opposite side. Figure 2.1 shows the schematic representation of periodic boundary conditions for a system in 2 dimensions.

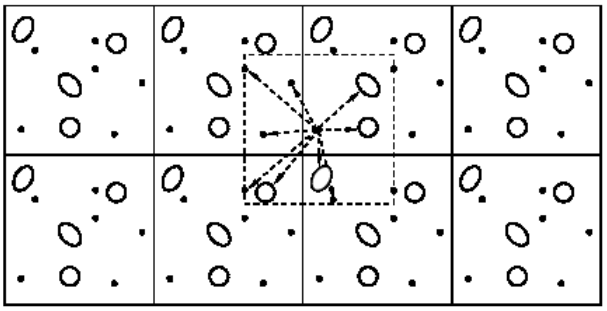

FIGURE 2.1: Schematic representation of periodic boundary conditions (taken from page 34 of [2])

The application of periodic boundary conditions limits the observations where long wavelength fluctuations are expected to be important, for instance near the continuous phase transition because the longest wavelength that can be observed in simulation can be equal to the length of the box.

Because of application of periodic boundary conditions, each particle interacts with all other particles not only in the primary simulation box but even outside in all other boxes including the self-images of the particle. This makes the calculation of interactions (an infinite sum) difficult. Since many systems have short-range interactions [6] and in that case, we can apply a scheme called *minimum image convention* (discussed next) which makes application of periodic boundary conditions effective.

Minimum Image Convention For short-range interactions, the intermolecular potentials can be cutoff beyond a certain length r_c. The case of r_c less than half the length of the box makes application of periodic boundary conditions effective. Because in such case, one needs to consider the interaction of a particle with the nearest periodic image of any other particle (see dotted box in Fig. 2.1).

[6] Long-range interactions like Coulomb and dipolar interactions need special treatment so that interactions from periodic images are taken account explicitly. One such method is Ewald sum.

The most popular way to cutoff the interaction in MD simulations is to truncate the potential and then shift it such that is vanishes at cutoff radius:

$$u_{cut}(r) = \begin{cases} u(r) - u(r_c) & : r \leq r_c \\ 0 & : r > r_c \end{cases}$$

This way of truncation and shifting of potential makes potential smooth but one needs to consider pressure and potential energy tail corrections [2] [5] . Also, one should be careful if the interactions are anisotropic [7]. In such cases, the truncation of potential should be at a point where the pair potential has a fixed value.

2.1.6 Neighbour List

As we discussed in last section 2.1.5 that if we put a cutoff (smaller than the length of simulation box) on the range of interaction then many pairs don't contribute to the energy calculation. But in order to check whether a pair contributes or not, it is necessary to calculate the pair separation which is the most time-consuming part of almost any MD simulation. So, it will be efficient to apply some technique such that the pairs which don't contribute to the energy of the particle could be exempted from computing the separation. Such techniques improve the performance of the simulation significantly. One of such techniques is Verlet list or neighbor list [17]. Here we consider an another cutoff radius r_v slightly bigger than r_c (see 2.1.5) and associate a list (called Verlet list or neighbor list) of particles to each particle in the simulation box. To make the list for any particle i, only those particles are put in the list which is within r_v with respect to particle i. Now while calculating the interactions, only those particles are considered which are in the list. We don't rebuild the next neighbor list until the maximum displacement of the particles in the list is greater than $r_v - r_c$ (called skin width). In this way, we get the advantage that there is no need to calculate all the separations not contributing to energy, at least for few number of time steps.

There is another technique called cell list or linked-list which performs the similar job as Verlet list. Here the simulation box is spatially divided into virtual cells

[7] This point should be considered for Lennard-Jones mixture

with a size equal to slightly greater than the cutoff radius r_c. Each particle in a given cell interacts with only those particles in the same or neighboring cells. In this way, the number of iterations needed to calculate the force is reduced. Cell list method is very useful when one writes a parallel MD program. Generally, neighbor list scheme is more efficient than cell list but sometimes people use a scheme which is the combination of the two list.

2.2 Introduction to Non-equilibrium Molecular Dynamics

In the previous section, we discussed the technique of MD for equilibrium systems where there are no thermodynamic fluxes present in the system. In this section, we extend the technique to non-equilibrium systems so that non-equilibrium ensembles could be sampled. One important reason for this extension is that here the calculation of transport coefficients is possible beyond the linear regime. The computation of transport coefficients is even possible by measuring time correlation functions as discussed in section 1.1.2. This is possible because time correlation functions and transport coefficients are related under linear response theory via the dynamic fluctuation-dissipation theorem [18]. The idea behind this theorem is that particles in an equilibrium system diffuse and by studying the dynamics of the diffusion, transport quantities can be estimated. One big disadvantage of such method which measures transport properties is that diffusion is generally a very slow process in equilibrium systems which makes the measurement of transport coefficients difficult. Hence it is useful to apply some field or perturbation such that much larger fluctuation may be induced and then measure the response of the system by keeping track of the motion of the particles. Here the measurements of quantities like pressure or temperature, are done in the same way as in equilibrium MD. Also in order to avoid surface effects, the system is designed such that it becomes consistent with periodic boundaries or sometimes boundaries are modified to preserve translational invariance and periodicity. In non-equilibrium molecular dynamics (NEMD), at first the perturbation is switched on and long-time steady-state responses may then yield transport coefficients. Sometimes periodically oscillating perturbations are also

applied. Now we consider the thermal perturbation of an atomic system in order to measure different quantities associated with the system.

2.2.1 Response to Applied Thermal Perturbation

One important quantity in a thermally perturbed system is the heat current density $\mathcal{J}$ which can be computed in NEMD simulation using the following formula:

$$\mathcal{J} = \frac{1}{V}\left[\sum_{i=1}^{N} e_i \mathbf{v}_i - \sum_{i=1}^{N} \mathbf{S}_i \mathbf{v}_i\right] \tag{2.12}$$

where V is the volume containing N particles, e_i is the total energy (kinetic+potential) per atom, $\mathbf{v}_i$ is the velocity of ith atom and $\mathbf{S}_i$ is the per atom stress tensor. In matrix form it can be written as [6] [19]:

$$\begin{pmatrix} \mathcal{J}_i^x \\ \mathcal{J}_i^y \\ \mathcal{J}_i^z \end{pmatrix} = \frac{1}{V}\left[\begin{pmatrix} e_i - S_i^{xx} & -S_i^{xy} & -S_i^{xz} \\ -S_i^{yx} & e_i - S_i^{yy} & -S_i^{yz} \\ -S_i^{zx} & -S_i^{zy} & e_i - S_i^{zz} \end{pmatrix} \begin{pmatrix} \mathbf{v}_i^x \\ \mathbf{v}_i^y \\ \mathbf{v}_i^z \end{pmatrix}\right] \tag{2.13}$$

Stress tensor is symmetric i.e., $S^{\alpha\beta} = S^{\beta\alpha}$ and it is defined as,

$$S^{\alpha\beta} = -\frac{1}{2}\sum_{i \neq j}(x_i^\alpha - x_j^\alpha) f_{ij}^\beta \tag{2.14}$$

Here $\alpha, \beta \in \{x, y, z\}$, i and j are particle index and f_{ij}^α is the αth component of the force on atom i due to j. The numerical implementation of heat current density has been done in section 3.3.

Chapter 3

Modeling and Results

This chapter talks about the details of the computer simulation performed. At first, we present the details of the model on which simulation has been done. The whole work has been divided into equilibrium simulation and non-equilibrium simulation. We also discuss the method and results of each simulation.

3.1 Details of the Model and Simulation

Here we perform molecular dynamics simulation of an 80:20 $\langle A : B \rangle$ binary mixture of particles that interact via Lennard-Jones potential given by,

$$V_{\alpha\beta} = 4\epsilon_{\alpha\beta}\left[\left(\frac{\sigma_{\alpha\beta}}{r}\right)^{12} - \left(\frac{\sigma_{\alpha\beta}}{r}\right)^{6}\right] \tag{3.1}$$

where α, β refer to the two particles A and B respectively, in the mixture. For the particular mixture which we have considered, the constants $\epsilon_{\alpha\beta}$ and $\sigma_{\alpha\beta}$ are given by $\epsilon_{AA} = 1.0$, $\sigma_{AA} = 1.0$, $\epsilon_{AB} = 1.5$, $\sigma_{AB} = 0.8$, $\epsilon_{BB} = 0.5$ and $\sigma_{BB} = 0.88$. Also, the potential is cut off and shifted at a distance $2.5\sigma_{\alpha\beta}$. We state all the results in reduced units (for details see Appendix A) with ϵ_{AA}, σ_{AA} and $\sqrt{\sigma_{AA}^2/\epsilon_{AA}}$ as the unit of length, energy and time, respectively. All particles are of mass unity.

The simulation is done with N particles in a rectangular box of dimension L_x, L_y and L_z. We have always considered the system at density 1.2 but system size N and hence box dimensions vary in different simulations.

This binary mixture is a model glass-former, called Kob-Andersen binary Lennard-Jones mixture [20] [4] [3], which has been studied extensively in last few years. At this density and low temperatures, the slow dynamics of the mixture is well described by the mode-coupling theory with a critical temperature $T_c \approx 0.435$ called mode-coupling temperature. At temperatures below T_c the relaxation time of the system becomes very high ($\mathcal{O}(10^7)$ time units). Hence, T_c provides a reference threshold temperature where equilibrium dynamics can be explored in computer simulations.

The equations of motion have been numerically integrated using the velocity form of Verlet algorithm with a step size of $dt = 0.005$. Always the periodic boundary conditions have been applied. Since, most of the time, we are interested in the low temperature behavior of the mixture, so whenever simulation is started, the system is at first equilibrated at some higher temperature (say at $T = 3.0$) and then it is quenched to lower temperatures T_f to proceed with the simulation. Temperatures have been controlled using Berendsen thermostat for equilibrium simulations while Langevin thermostat has been used for non-equilibrium simulations.

3.2 Equilibrium Simulation

In this section, we discuss the details of the simulation performed with binary Lennard-Jones mixture under NVE condition. We have calculated the equilibrium properties like pressure, total energy (E_{tot}), potential energy (E_{pot}) at different temperatures. We have shown the different pair correlation functions $g_{\alpha\beta}(r)$ for AA and BB correlation and the dependence of mean squared displacement $\langle r^2(t)\rangle$ (MSD) for A-type particles at different temperatures. We also measure the overlap function $Q(t)$. Finally, we discuss: what happens when the system is quenched below mode-coupling temperature?

3.2.1 Simulation Method

Here we consider $N = 1000$ particles (800 A-type and 200 B-type). At density 1.2 the dimension of the box comes out to be $L_x = L_y = L_z = 9.41$. As mentioned in the last section, a fully equilibrated system at relatively higher temperature

$T = 5.0$ is quenched to a lower temperature T_f using the Berendsen thermostat for a period at least ten times of relaxation time [1] of the system at the temperature T_f. After this period, the system is set free at constant energy for another period of the same length. Now instantaneous potential energy and temperature of the system are observed for some time, if it does not show any drift then this final state is considered to be a representative equilibrium state of the system at temperature T_f, and also this final state serves as the initial configuration for further simulation (production phase) at constant energy. We now start collecting the samples of different quantities (like total energy, potential energy, temperature) at some interval of few time steps (say 500 steps). We collect sufficient number of samples such that they produce statistically acceptable results after averaging.

The simulation is performed for following T_f's: 5.0, 4.0, 2.0, 1.0, 0.80, 0.70, 0.60, 0.55, 0.50, 0.475, 0.466, 0.45.

3.2.2 Simulation Results

In this part, we discuss the results produced in the simulation. Fig. 3.1, 3.2 and 3.3 show the variation of the potential energy, the total energy and the pressure respectively as a function of temperature. Since we have done many simulations at low temperatures, so these quantities have been plotted with inverse temperature $(\frac{1}{T})$. It can be clearly seen from these plots that the three quantities decrease with the decrease in temperature. The most important observation that can be made is, these quantities don't show any sign of anomalous behavior, at least, for the temperatures which have been considered. This implies, the system during these simulations, is always in equilibrium and it has not undergone any glass transition for the cooling rates used [3].

In Fig. 3.4 we show the variation of radial distribution function $g_{\alpha\beta}(r)$ for α, $\beta \in \{A, B\}$ at temperature $T = 1.0$. Here the plots for AA correlation and BB correlation are very much different from each other. The reason for this difference may be due to the fact that B-type particles are less in number and

[1] relaxation time [21] for higher temperatures close to $T > 1.0$ is of the order of 10 but it increases dramatically as lower temperatures are approached. For temperature near 0.5, it is of the order of 10^3.

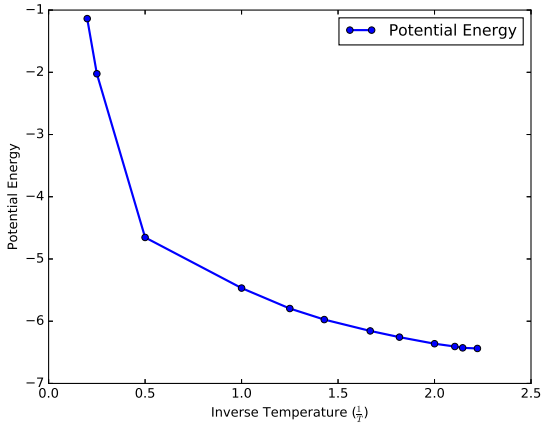

FIGURE 3.1: Potential energy dependence on temperature for a system of $N = 1000$ particles in a box of $L_x = L_y = L_z = 9.41$ [3].

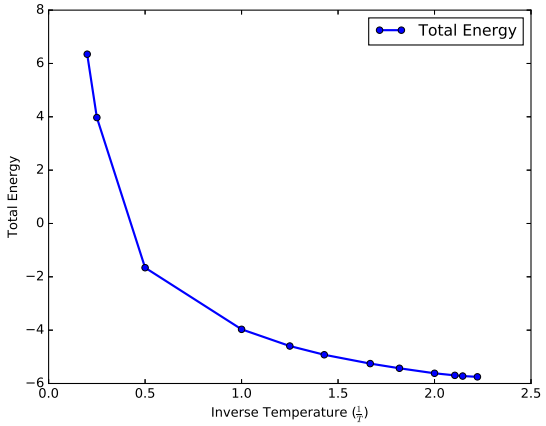

FIGURE 3.2: Total energy dependence on temperature for a system of $N = 1000$ particles in a box of $L_x = L_y = L_z = 9.41$ [3].

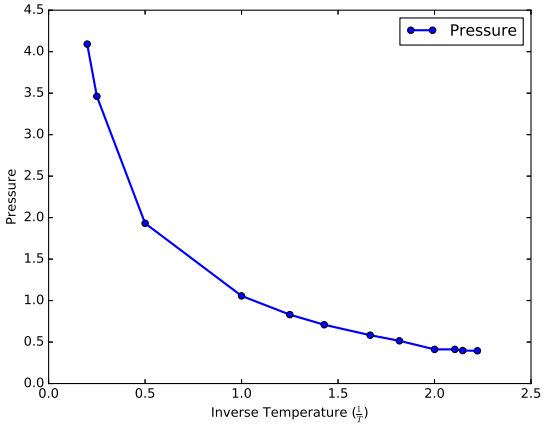

FIGURE 3.3: Pressure dependence on temperature for a system of $N = 1000$ particles in a box of $L_x = L_y = L_z = 9.41$ [3].

their radius being smaller than A-type particles. The first highest peak for AA correlation occurs near $r = 1$ but for BB correlation it is near $r = 1.5$.

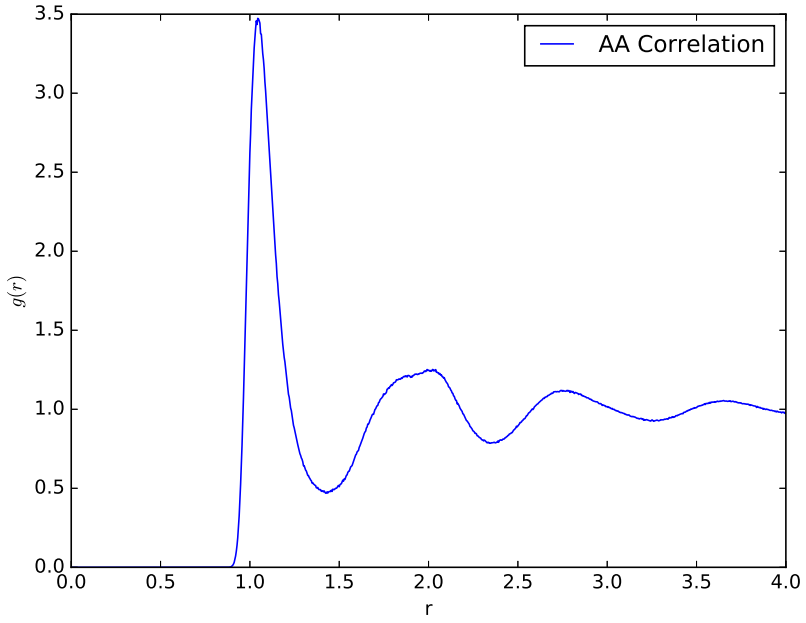

(a)

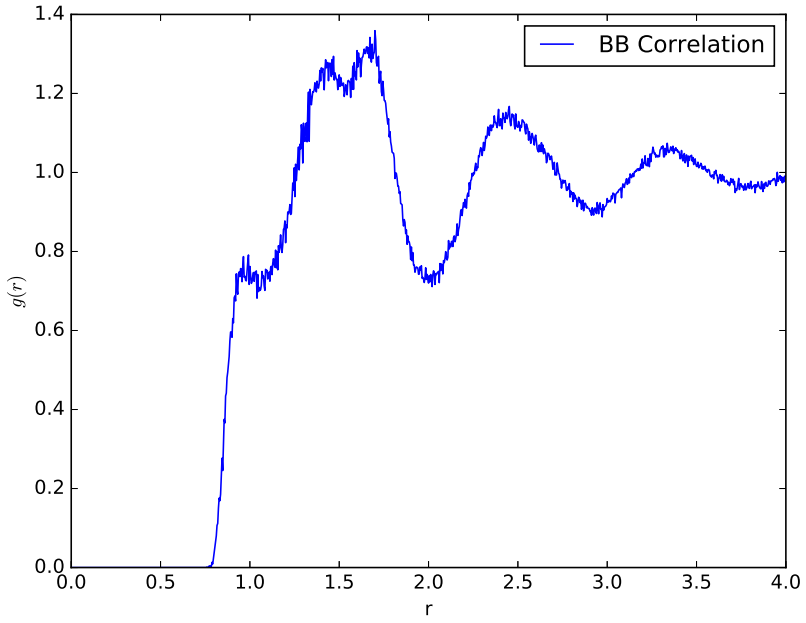

(b)

FIGURE 3.4: Radial distribution function $g(r)$ for (a) AA and (b) BB correlation for $N = 1000$ particles at temperature $T = 1.0$ [3].

Now we show the behavior of two time dependent quantities, mean squared displacement $\langle r^2(t)\rangle$ of a tagged particle and the overlap function $Q(t)$ for different temperatures. Fig. 3.5 shows MSD (1.1.2) of A-type particles as a function of time in a log-log plot. We can see from the plots that for short times the behavior is power law with exponent 2 i.e., t^2, which represents the ballistic motion of the particles. The long time dependence is linear which shows diffusive behavior. These two regimes are separated by a plateau like curve (MSD changes slowly) which indicates that the motion of particles is very slow for some time. For lower temperatures, the plateau regime extends for longer range of time. Overall the MSD curves tell that the dynamics of the system is very different on different time scales. Also, the diffusion coefficient which is determined from the long time behavior of MSD, decreases with the decrease in temperature.

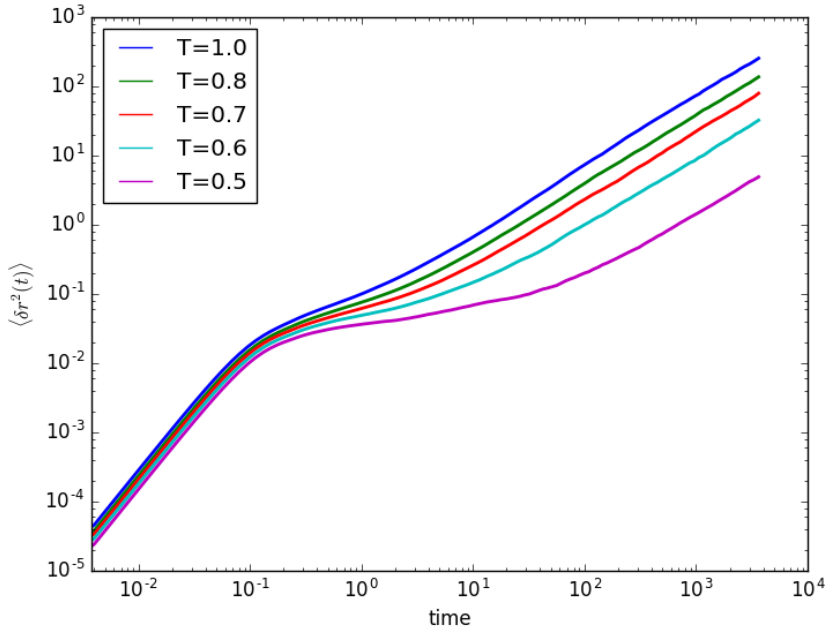

FIGURE 3.5: Time dependence of mean squared displacement $\langle \delta \mathbf{r}^2(t)\rangle$ for A-type particles for a range of temperatures.

Fig. 3.6 shows the overlap function Q(t) (1.1.2) as a function of time. It has been measured by considering the window function $w(r) = 1$ if $r \leq a$ with $a = 0.3$ and zero otherwise. Here it can be clearly seen that for lower temperatures the system is relaxing much slowly. Also if we compare the time taken by the system to relax at different temperatures then we find that this time keeps on increasing as we go towards lower temperatures. Clearly the relaxation time is very large at $T = 0.5$ compared to that at $T = 0.6$.

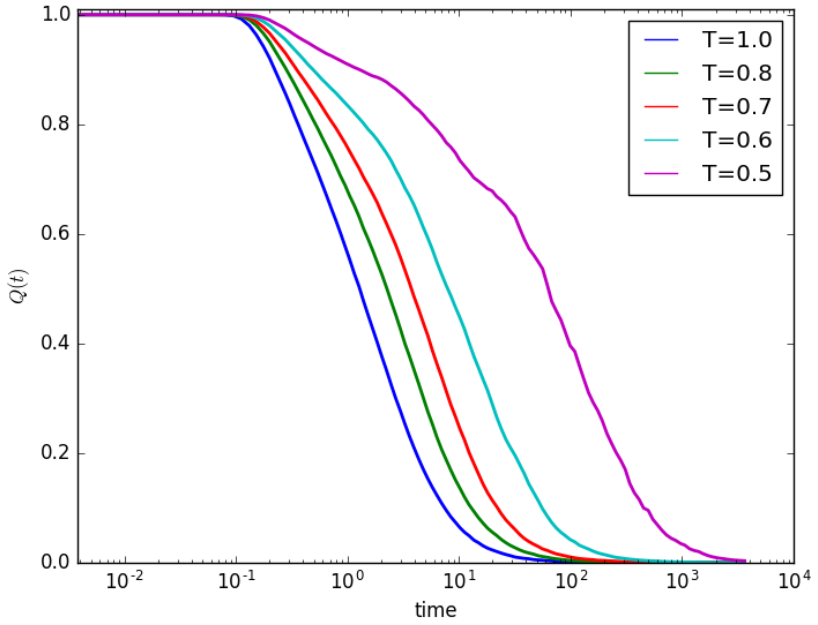

FIGURE 3.6: Time dependence overlap function $Q(t)$ for a range of temperatures.

3.2.3 Quenching below the Mode-Coupling Temperature

As discussed previously, the equilibrium dynamics of the system is well described by the mode coupling theory [22] (MCT) with a critical temperature $T_{MCT} \approx 0.435$. But when the system is quenched below this critical temperature, there is an increase of many orders of magnitude in the viscosity of the liquid [1] and there is a huge increase in the relaxation time. Because of slow dynamics, the response of the system becomes so slow that it runs out of equilibrium. If any property of the system is measured, it depends on the point of time where the property has been measured, which happens due to the aging of the system. We have tried to show this non-equilibrium behavior in Fig. 3.7. Here the system has been quenched from a relatively higher temperature $T = 3.0$ to lower temperatures $T = 0.5$ and $T = 0.3$. The behavior of potential energy for the two cases has been shown in the figure. In the zoomed figure Fig. 3.7 (b) it is clear that for quenching to $T = 0.3$ the potential energy keeps on decreasing in contrast to the another case of quenching to $T = 0.5$ where potential energy fluctuates about some mean value.

Figures 3.8 and 3.9 show the time dependence of two quantities, MSD $\langle r^2(t) \rangle$ and overlap function $Q(t)$ (measured by considering the window function $w(r) = 1$

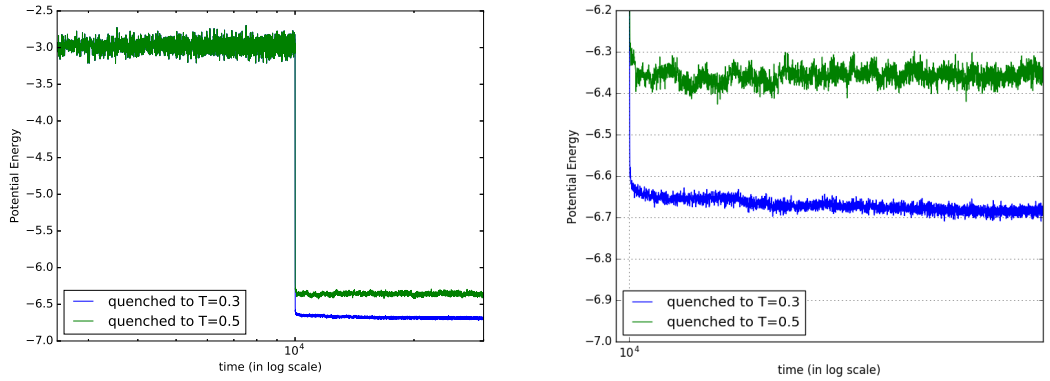

(a) (b)

FIGURE 3.7: Potential energy dependence comparison for a system of $N = 1000$ particles with density 1.2, quenched from $T = 3.0$ to $T = 0.5$ and $T = 0.3$.

if $r \leq a$ with $a = 0.3$ and zero otherwise), for different waiting times t_w (i.e. the time elapsed since quench). We clearly see in MSD plot, as the system gets older the plateau region keeps on extending and the long time behavior does not reach linear regime within the observational time limit. This means, the system's dynamics gets slower with increasing age and is non-diffusive.

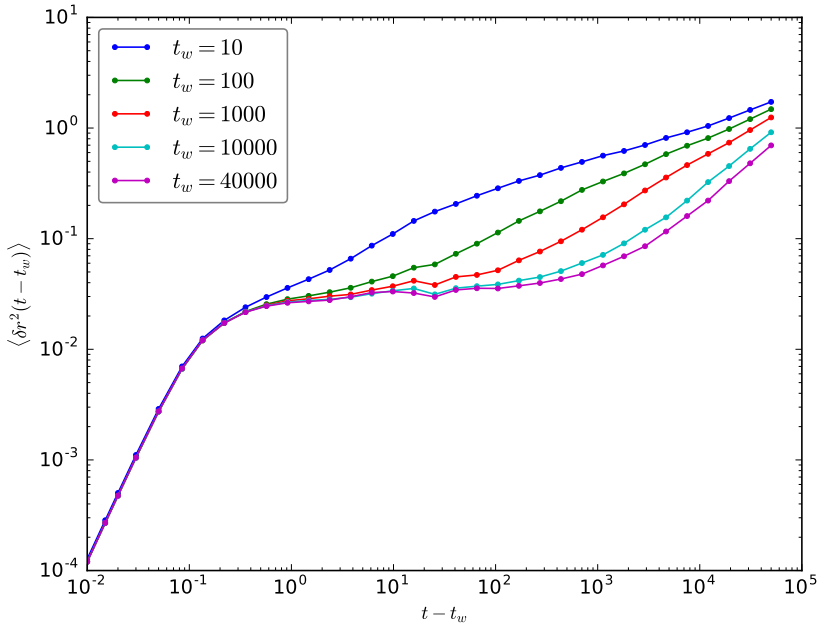

FIGURE 3.8: Dependence of mean squared displacement $\langle r^2(t) \rangle$ on time with changing age t_w, for a system of $N = 22500$ particles at density 1.2 quenched from $T = 3.0$ to $T = 0.4$.

From Fig. 3.9 it evident that the relaxation of the system slows down with increasing age. The older system has even not relaxed within the observational time limit. This strongly supports our assumption that the dynamics in glassy state becomes slower with increasing age.

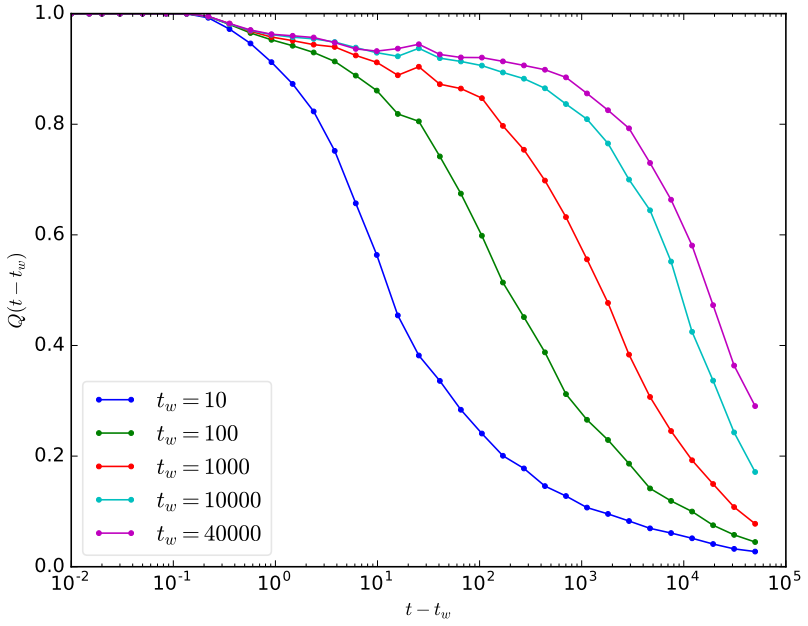

FIGURE 3.9: Time dependence of overlap function $Q(t)$ with changing age t_w, for a system of $N = 22500$ particles at density 1.2 quenched from $T = 3.0$ to $T = 0.4$.

3.3 Non-equilibrium Simulation

This section discusses the details of the simulation done with the binary Lennard-Jones mixture under non-equilibrium situation due to a temperature gradient (following sections describe) in the z-direction along the length L_z of the system. We have studied the different properties of the system when a non-equilibrium steady state is maintained. We have calculated the local temperature profile which has been setup in the system. We have also calculated the local heat current density along the system. We have investigated the nature of local number density of all particles and A-type particles.

3.3.1 Simulation Method and Measurements

We consider $N = 22500$ particles (18000 A-type and 4500 B-type) in a rectangular box of dimension $L_x = L_y = 14.12$ and $L_z = 94.10$. The cross-sectional area is $L_x \times L_y$. We also assume periodic boundary conditions along all three orthogonal directions. At first we prepare a fully equilibrated system at a mean temperature T_m by following the process discussed in previous sections. Then in order to maintain a temperature gradient along z-direction, we thermostat a region (cold region COLD or sink) of width $L_z/10$ in middle at lower temperature T_c and another two regions of width $L_z/20$ (hot region HOT or source) each at two extreme ends at higher temperature T_h (see Fig. 3.10). The temperatures T_h and T_c have been chosen symmetrically about the mean temperature T_m.

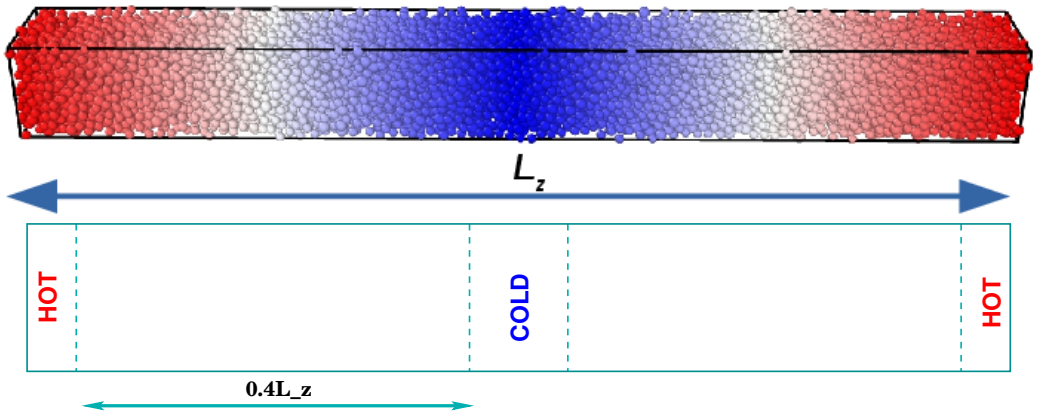

FIGURE 3.10: Schematic diagram of the system of length L_z along z with cross-sectional area $L_x \times L_y$, where red colour represents hotter region while blue represents colder region. The two hot regions (HOT) of width $L_z/20$ each along z at extreme ends is thermostated at temperature T_h and a cold region (COLD) of width $L_z/10$ along z at middle is thermostated at temperature T_c. There exists a spatial temperature gradient defined as $dT/dz = (T_h - T_c)/L'_z$ along z in the two regions of width $L'_z = 0.4L_z$ each between HOT and COLD.

Since there is a temperature difference between source and sink, we expect a continuous variation of temperature along z in the two regions of dimension $L_x \times L_y \times 0.4L_z$ each between the thermostated regions HOT and COLD (see Fig. 3.10). The temperature gradient is defined as $dT/dz = (T_h - T_c)/L'_z$ where $L'_z = 0.4L_z$. By varying T_h and T_c, the temperature gradient along the system can be varied. The thermostating of the hot and the cold regions has been done using Langevin thermostat. We wait for a period of at least 5×10^4 until a non-equilibrium steady state is maintained. We ensure this steady state situation by monitoring the spatial profile of local temperature T_i and z-component of heat

current density $\mathcal{J}_i^z$ established along the system. In steady state situation, the temperature profile should show a linear spatial temperature variation from T_h to T_c and the heat current density should fluctuate about some mean value in the regions between HOT and COLD. Local quantities have been measured by binning the simulation box along z into 40 partitions, labeled $i = 1, ..., 40$, and then separately averaging the 5×10^4 samples collected at an interval of 500 time-steps in each bin. In order to have more statistically sensible data, the final results have been averaged over many independent runs of simulation.

Simulation has been performed at different mean temperatures T_m and for each mean temperature different temperature gradients have been considered by varying T_h and T_c symmetrically about T_m as discussed above. We have calculated following quantities in the simulation: spatial profile of local temperatures T_i, z-component of heat current density $\mathcal{J}_i^z$, local number density of all particles n_i, local number density of A-type particles nA_i,local ratio of number of A-type particles to all particles N_{Ai}/N_i and the variation of heat exchanged per unit time $\mathcal{H}/t$ between HOT and COLD reservoirs with temperature gradient dT/dz.

Now let's discuss the details of the calculation of each quantity in detail. As mentioned previously, we have 40 bins of L_z (labeled $i = 1, ..., 40$) and each quantity has been measured in each bin, after passing the initial transient period.

- Local temperature T_i is measured in each bin at regular intervals of time and then averaged separately. Finally, the averaged data is plotted along the system in the z-direction.
- Similarly, the local heat current density $\mathcal{J}_i^z$ is measured using the formula in equation 2.12, averaged and plotted.
- For local number density profile of all particles and number profile of A-type particles, corresponding numbers N_i (number of all particles in ith bin) and N_{Ai} (number of A-type particles in ith bin) in each bin are counted. After sufficient averaging, N_{Ai} corresponding to each bin is plotted along the system but for number density profile, each N_i is separately divided by the volume of each bin $\mathcal{V} = L_x \times L_y \times L_z/40$ i.e., $n_i = N_i/\mathcal{V}$ and then plotted along the system.
- Finally to plot the variation of heat exchanged per unit time $\mathcal{H}/t$ between HOT and COLD reservoirs with temperature gradient dT/dz, we calculate

the net amount of heat $\mathcal{H}$ transferred from the HOT reservoir to COLD reservoir during a time t ($= 1.25 \times 10^5$) for different temperature gradients at a given mean temperature T_m.

3.3.2 Results

At first, we present the role of damping parameter (τ_d) used for thermostating via Langevin thermostat to the hot and cold regions. If damping parameter is larger then it means thermostating is slow while smaller damping parameter implies vigorous thermostating. Here we have considered $T_m = 0.5$, $T_h = 0.525$ and $T_c = 0.475$ with following damping parameters: 0.05, 0.5, 5.0, 10.0. We have plotted the spatial profile of local temperatures T_i and z-component of heat current density $\mathcal{J}_i^z$ calculated in the 40 bins along z of the system.

It can be clearly seen in the plots (Fig. 3.11) that if τ_d is larger like $\tau_d = 5$ or 10, then temperature profile and current density profile are not consistent. The temperature of the hot and cold reservoirs are not maintained at the target temperatures. Also if τ_d is too small like $\tau_d = 0.05$, then current density shows large fluctuations. But damping parameter having some intermediate value like $\tau_d = 0.5$, seems to be good. Hence, in further simulations throughout we have done the thermoststing with damping parameter $\tau_d = 0.5$.

Now we present the plots for the simulations performed for the system at three mean temperatures, at relatively higher temperature $T_m = 1.0$ (Fig 3.12), a temperature slightly above mode coupling temperature $T_m = 0.5$ (Fig 3.13) and a temperature below mode coupling temperature $T_m = 0.3$ (Fig 3.14).

Now let's discuss these plots and see, what conclusions can we make out of it.

- For the simulation performed at three different mean temperatures $T_m = 1.0, 0.5, 0.3$, a very good temperature profile has been setup. The temperature of the HOT and COLD regions have been very close to desired values T_h and T_c.
- The heat current density $\mathcal{J}_i^z$ at the three mean temperatures for different temperature gradients $\frac{dT}{dz}$ show a regular behavior. For a given mean temperature, the magnitude of heat current density increases with the increase

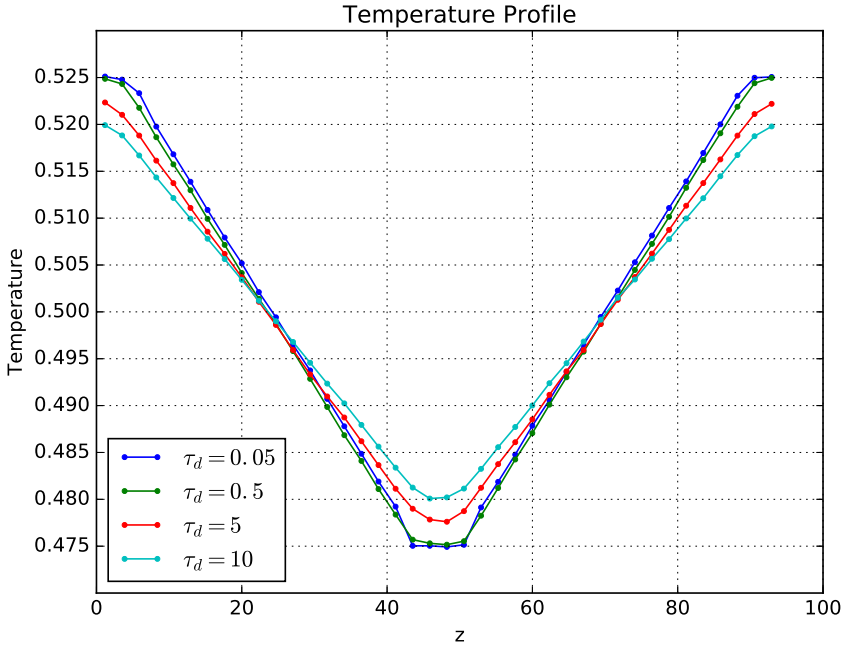

(a)

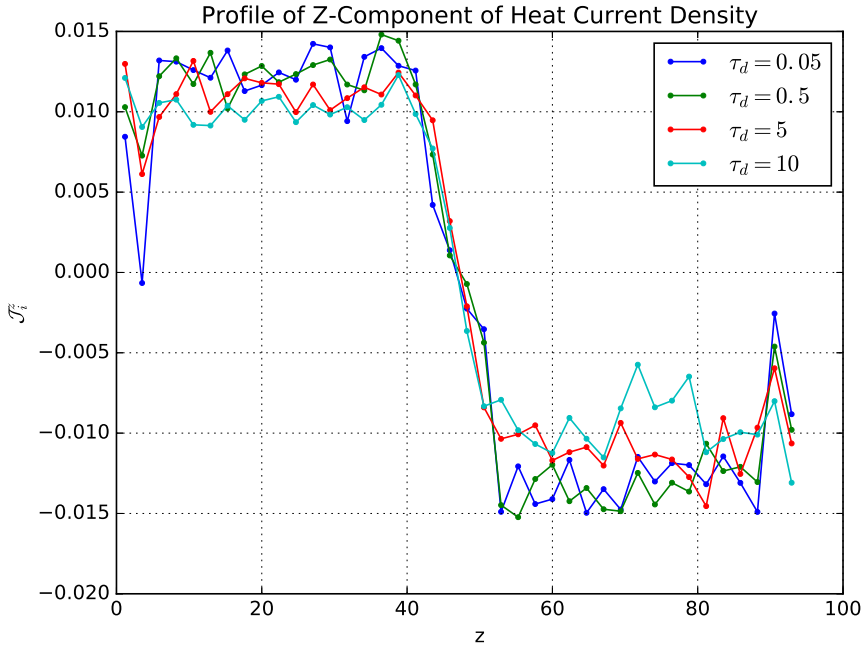

(b)

FIGURE 3.11: Effect of damping parameter on (a) temperature profile and (b) local heat current density at a mean temperature of $T_m = 0.5$ with $T_h = 0.525$ and $T_c = 0.475$. Total number of particles used in simulation is $N = 22500$ inside a box with $L_x = L_y = 14.12$ and $L_z = 94.10$.

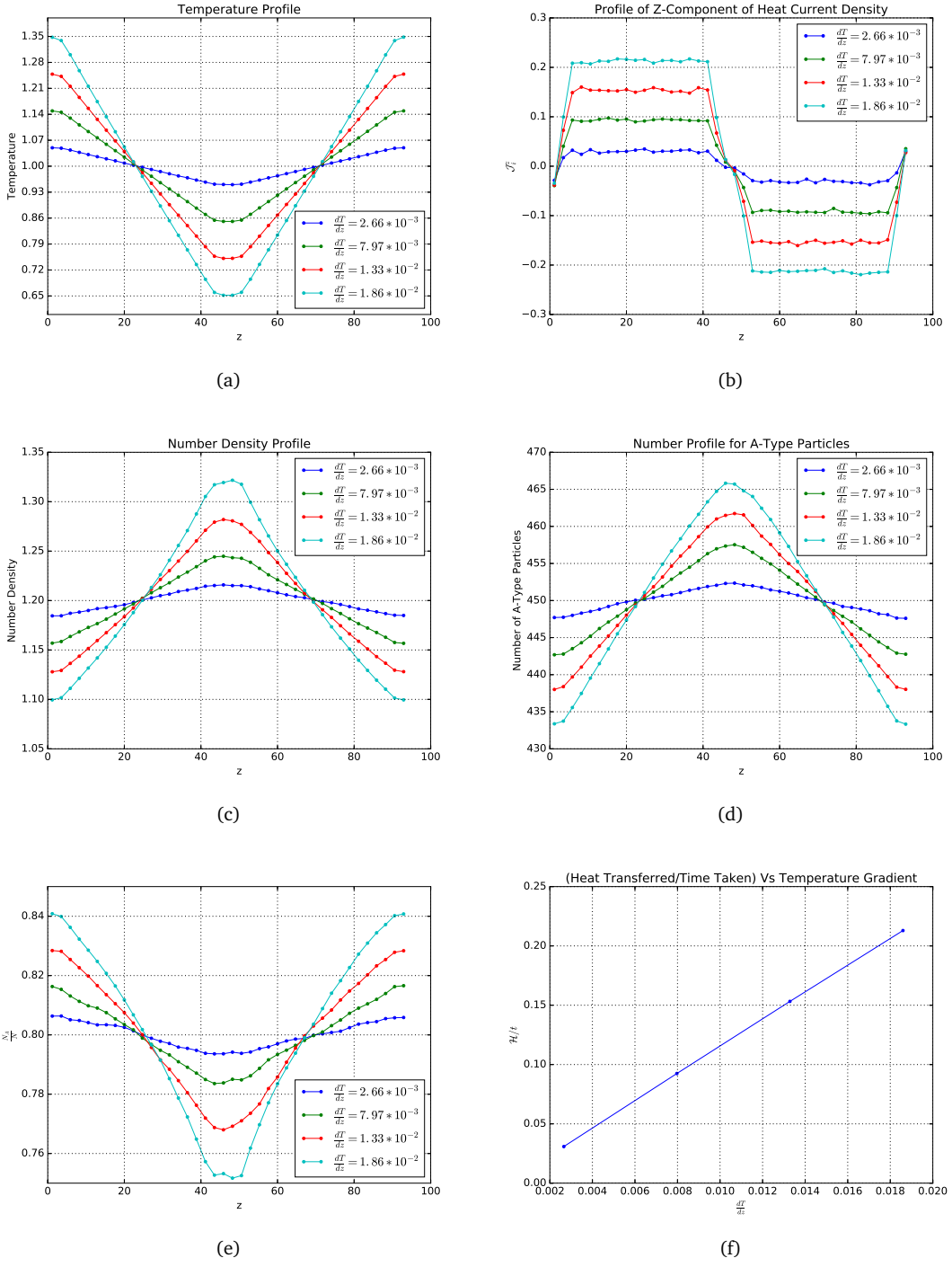

FIGURE 3.12: Plot of (a) temperature profile, (b) local heat current density, (c) local number density of all particles, (d) local number density of A-type particles and (e) local ratio of number of A-type particles to all particles, along the system, at a mean temperature of $T_m = 1.0$. (f) Variation of heat exchanged per unit time $\mathcal{H}/t$ between HOT and COLD reservoirs with temperature gradient dT/dz at mean temperature $T_m = 1.0$. Total number of particles used in simulation is $N = 22500$ inside a box with $L_x = L_y = 14.12$ and $L_z = 94.10$.

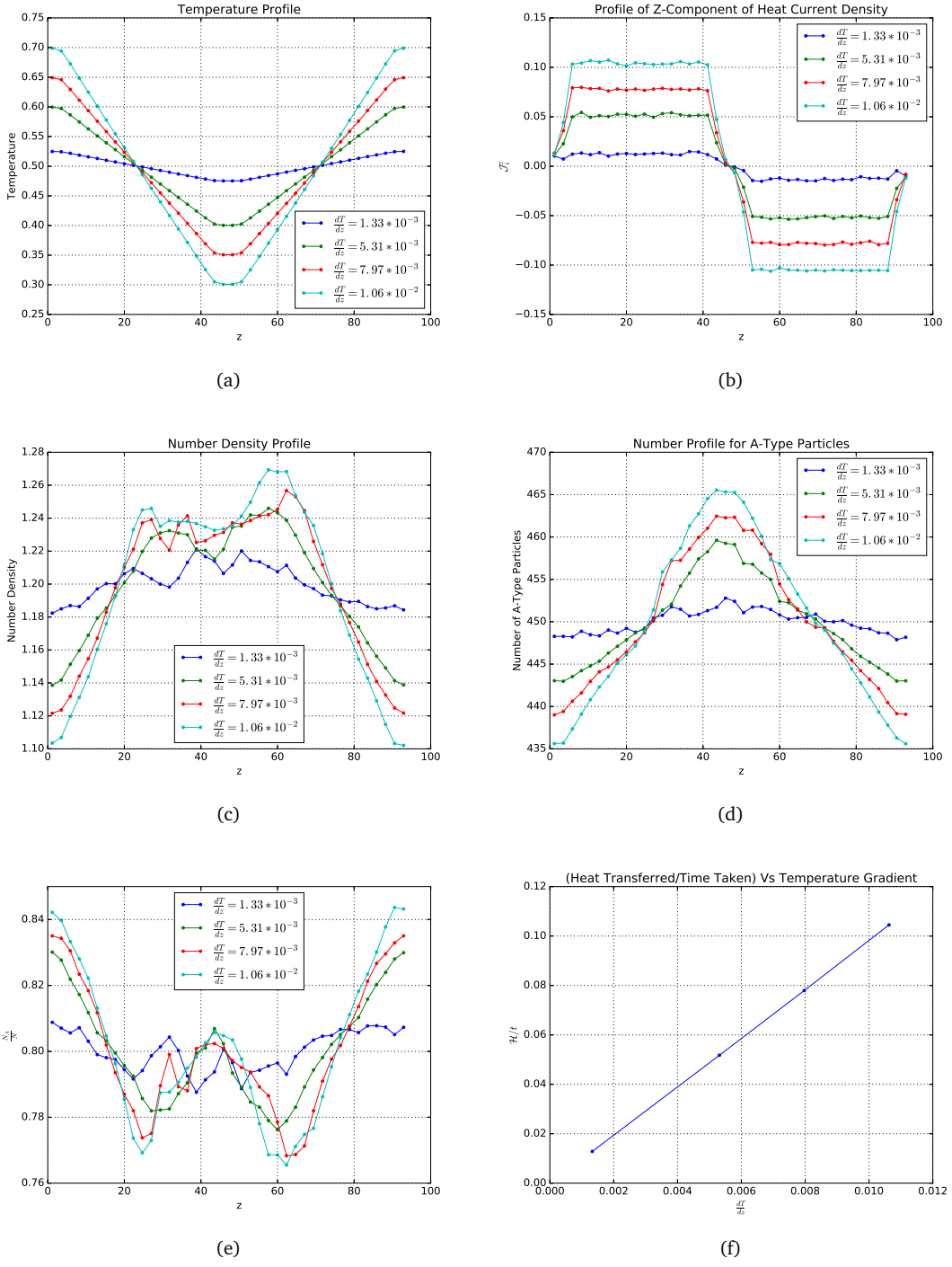

(a) (b) (c) (d) (e) (f)

FIGURE 3.13: Plot of (a) temperature profile, (b) local heat current density, (c) local number density of all particles, (d) local number density of A-type particles and (e) local ratio of number of A-type particles to all particles, along the system, at a mean temperature of $T_m = 0.5$. (f) Variation of heat exchanged per unit time $\mathcal{H}/t$ between HOT and COLD reservoirs with temperature gradient dT/dz at mean temperature $T_m = 0.5$. Total number of particles used in simulation is $N = 22500$ inside a box with $L_x = L_y = 14.12$ and $L_z = 94.10$.

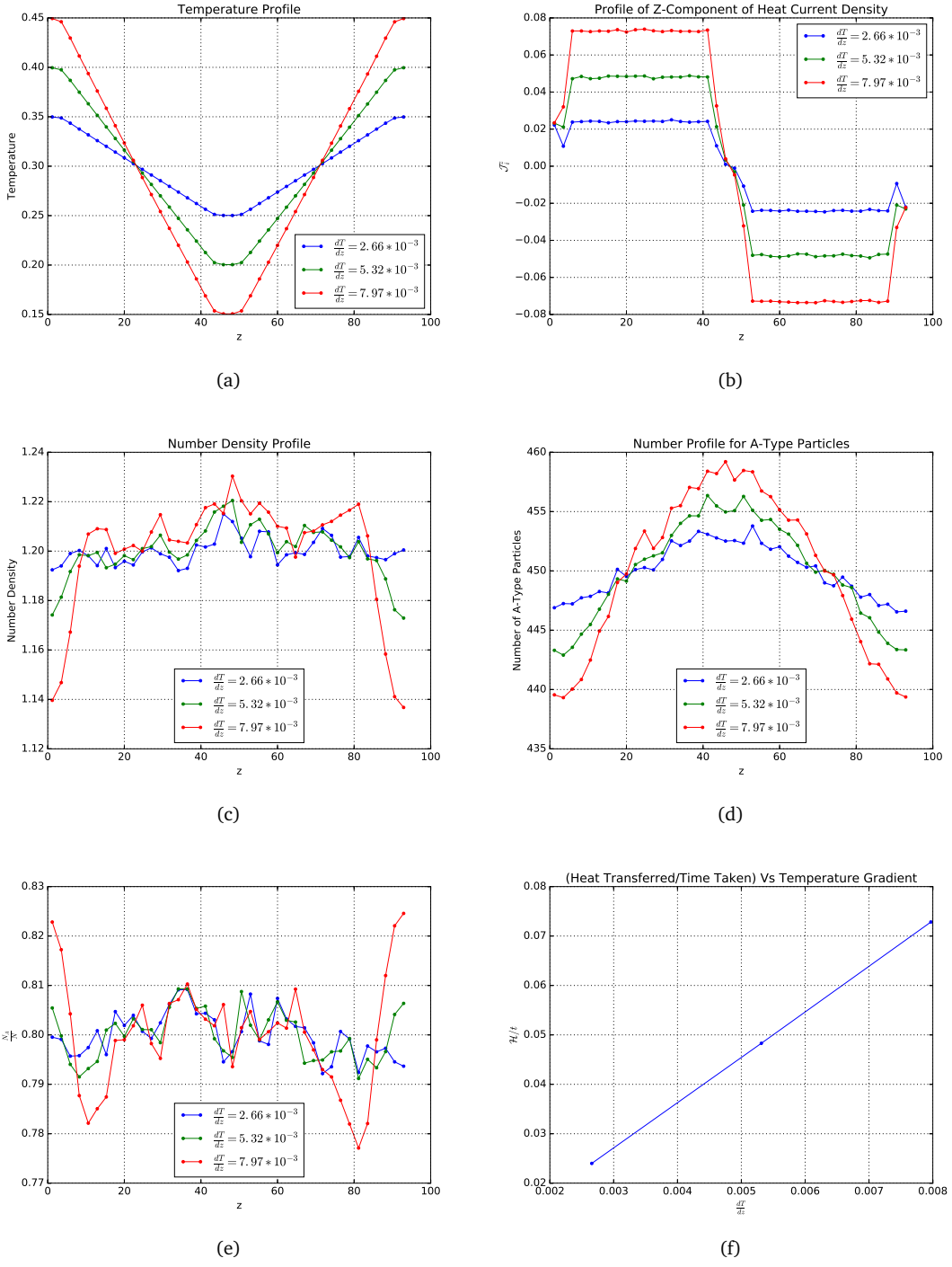

(a) (b)

(c) (d)

(e) (f)

FIGURE 3.14: Plot of (a) temperature profile, (b) local haet current density, (c) local number density of all particles, (d) local number density of A-type particles and (e) local ratio of number of A-type particles to all particles, along the system, at a mean temperature of $T_m = 0.3$. (f) Variation of heat exchanged per unit time $\mathcal{H}/t$ between HOT and COLD reservoirs with temperature gradient dT/dz at mean temperature $T_m = 0.3$. Total number of particles used in simulation is $N = 22500$ inside a box with $L_x = L_y = 14.12$ and $L_z = 94.10$.

in temperature gradient which is consistent with the Fourier's law of heat conduction while, for a given temperature gradient, the magnitude of heat current decreases with the decrease in mean temperature which indicates the dependence of thermal conductivity on the mean temperature.

- Number density profile for mean temperatures $T_m = 1.0$ has higher value near the region where temperature is higher, but for $T_m = 0.5$ (except for $\frac{dT}{dz} = 1.33 \times 10^{-2}$) and $T_m = 0.3$ the behavior is very much different. The most prominent reason for this unusual behavior seems to be the local temperatures for these cases, which lie in glassy regime.

- This unusual behavior is much more explicit when $\frac{N_A}{N}$ is observed. In this case, we observe two valleys each one place between the HOT and COLD regions.

- The number profile for A-type particles is almost regular for the three mean temperatures.

- The dependence of heat transferred per unit time $\mathcal{H}/t$ is linear on temperature gradient $\frac{dT}{dz}$ for the all three mean temperatures. The thermal conductivity of the material can be determined by estimating the slope of the linear plot.

Now we choose $T_h = 1.05T_m$ and $T_c = 0.95T_m$ for different T_m's: 0.5, 0.6, 0.7, 0.8, 0.9, 1.0; and plot the reduced temperature T_i/T_m profile along the system. Plots for different T_m's almost overlap each other (Fig. 3.15 (a)).This shows that a very good temperature profile has been build up for all the mean temperatures. We have also plotted the reduced number density profile $n_i/1.2$ where 1.2 is the density of system taken initially, for different mean temperatures (Fig. 3.15 (b)). Here, also almost all cuves overlap except $T = 0.5$ which may be due to low temperature case. Finally Fig. 3.15 (c) shows the variation of local heat current density $\mathcal{J}_i^z$ along the system for different mean temperatures. We can clearly see here that the magnitude of the z-component of heat current density increases with the increase in mean temperature which we also expect. These reduced plots show that the proerties of the system depend on temperature gradients not on mean temperatures.

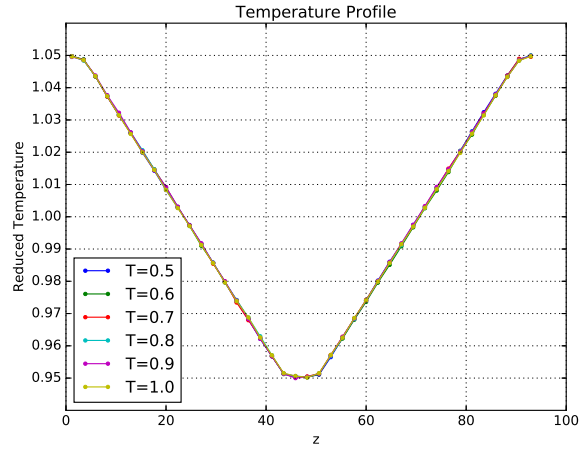

(a)

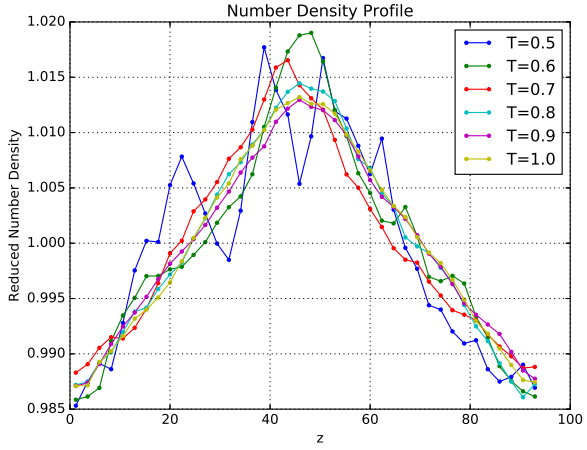

(b)

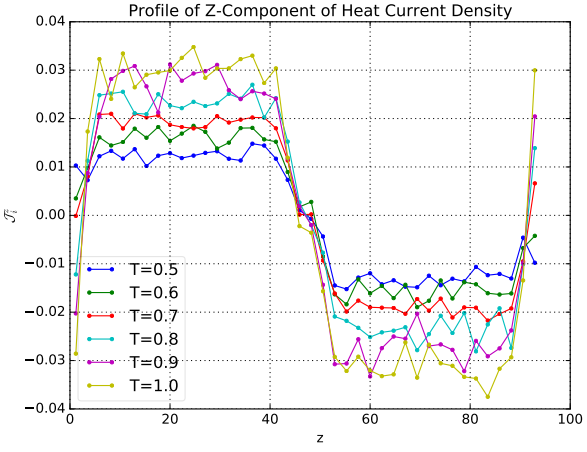

(c)

FIGURE 3.15: Plot of (a) reduced temperature profile T_i/T_m, where T_m is mean temperature, (b) reduced number density $n_i/1.2$ profile and (c) local heat current density $\mathcal{J}_i^z$ along the system for a range of mean temperatures. Simulation involves $N = 22500$ particles inside a box with $L_x = L_y = 14.12$ and $L_z = 94.10$.

Chapter 4

Conclusions and Future Directions

In this report, we mainly studied the behavior of a well-known model glass-former, Kob-Andersen binary Lennard-Jones mixture. We explored the properties of this glass-former under supercooled and glassy regime at a particular density 1.2 (in reduced units).

At first, we measured the different equilibrium properties of the model. The potential energy, total energy and pressure of the system were calculated at different temperatures lowest being $T_f = 0.45$. In the plots of these quantities, no any irregularity appeared which led us to the conclusion that at least for the cooling rates used in the simulation, the system is in full equilibrium. One can further conclude that any glass transition temperature for the model must be below $T = 0.45$. The study of mean squared displacement (MSD) $\langle \delta \mathbf{r}^2(t) \rangle$ and overlap function $Q(t)$ of the model at different temperatures also showed behavior identical to an equilibrium fluid. The MSD varied as t^2 (ballistic motion) for short range time and as t (diffusive behavior) for long range time. The plot for $Q(t)$ showed that the relaxation for the system is slower at lower temperatures.

Next, the system was quenched to a lower temperature $T = 0.3$ from some higher temperature. This quenching was compared with another quenching to $T = 0.5$. The potential energy curve showed a decreasing behavior for the case of quenching to $T = 0.3$ in contrast to the another case of quenching to $T = 0.5$ where potential energy showed fluctuation about some mean value. This led us to conclude that for the case of quenching to $T = 0.3$, the system is out of equilibrium. For this case, the overlap function and MSD showed different measurements at

different points of time. For MSD plot the plateau like region for the intermediate time range became wider indicating slower dynamics with increasing age and long time behavior was non-diffusive. The overlap function showed that the system relaxation slowed down with increasing age. This strongly supports our assumption that the dynamics in glassy state becomes slower with increasing age.

The final set of simulations that we performed was the study of the model glass former under external thermal perturbation. We established a temperature gradient in the z-direction along the length of the system by thermostating two different regions separated by some distance in the z-direction at two different temperatures. We performed simulations for various temperature gradients around three mean temperatures. We observed that a very good temperature profile was built and the magnitude of heat current density along z-direction increases with the increase in temperature gradient for a given mean temperature which is consistent with the Fourier's law of heat conduction. But for a given temperature gradient, the magnitude of heat current showed decrement with the decrease in mean temperature which indicates the dependence of thermal conductivity on the mean temperature. The local number density of all particles in mixture showed unusual behavior for temperatures in the glassy regime. The heat transferred per unit time showed linear dependence on temperature gradients for the all three mean temperatures.

This study can be further extended in many directions. The unusual behavior of local number densities for the temperatures in glassy regime needs to be probed with much more detail. The thermal conductivity of the system can be measured by extending the computations done here. The effect of aging can be studied in the non-equilibrium situation. Also, the future work should involve more extensive averaging, specially for obtaining definitive local density profiles, specially in the glassy regime.

Appendix A

Reduced Units

The use of reduced units makes easy to handle different quantities like temperature, density, pressure. In reduced units, a convenient unit of energy, length and mass are chosen and then all other quantities are expressed in terms of these basic units. With these, all quantities become dimensionless by dividing a typical length scale of the system. Another advantage of reduced units is, almost all quantities of interest are of order 1. This makes detection of errors easier in the simulation because if a quantity is very large or very small compared to 1 then this is a sign of an error in the simulation.

In Lennard-Jones system, the natural choice for basic units is σ the unit of length, $epsilon$ the unit of energy and m (the mass of atoms in the system) the unit of mass. All other units can be derived from these three basic units. For instance, in this reduced Lennard-Jones system the unit for time is $\sqrt{m\sigma^2/\epsilon}$ and for temperature is ϵ/k_B. Further, the Lennard-Jones potential in reduced units can be written as

$$V^*(r) = 4\left[\left(\frac{1}{r}\right)^{12} - \left(\frac{1}{r}\right)^{6}\right] \tag{A.1}$$

where, $V^*(r) = V(r)/\epsilon$ is the reduced potential. The quantities like pressure, density and temperature can be defined as reduced pressure $P^* = P\sigma^3\epsilon^{-1}$, reduced density $\rho^* = \rho\sigma^3$ and reduced temperature$T^* = Tk_B\epsilon^{-1}$. Another convenience that the reduced system of units provides that the same set of calculation can be used to study different systems, only we need to evaluate the basic units of the system under consideration.

The back translation of simulation results obtained in reduced units to real units can be done using basic reduced units. One such back translation for Lennard-Jones Argon is presented in the table below:

Quantity	Reduced Units	SI Units
Temperature	$T^* = 1$	$T = 119.8$ K
Density	$\rho^* = 1.0$	$\rho = 1680$ kg/m^3
Time	$\Delta t^* = 0.005$	$\Delta t = 1.09 \times 10^{-14}$ s
Pressure	$P^* = 1$	41.9 MPa

TABLE A.1: Table showing conversion between two system of units for Lennard-Jones Argon having following parameters: $\epsilon/k_B = 119.8$ K, $\sigma = 3.405 \times 10^{-10}$ m, Molar mass = 0.03994 kg/mol [2]

Bibliography

[1] M. D. Ediger, C. A. Angell, and Sidney R. Nagel. Supercooled liquids and glasses. *The Journal of Physical Chemistry*, 100(31):13200–13212, 1996. doi: 10.1021/jp953538d. URL http://dx.doi.org/10.1021/jp953538d.

[2] Daan Frenkel and Berend Smit. *Understanding molecular simulation: from algorithms to applications*, volume 1. Academic press, 2001.

[3] Walter Kob and Hans C. Andersen. Testing mode-coupling theory for a supercooled binary lennard-jones mixture. ii. intermediate scattering function and dynamic susceptibility. *Phys. Rev. E*, 52:4134–4153, Oct 1995. doi: 10.1103/PhysRevE.52.4134. URL https://link.aps.org/doi/10.1103/PhysRevE.52.4134.

[4] Walter Kob and Hans C. Andersen. Testing mode-coupling theory for a supercooled binary lennard-jones mixture i: The van hove correlation function. *Phys. Rev. E*, 51:4626–4641, May 1995. doi: 10.1103/PhysRevE.51.4626. URL https://link.aps.org/doi/10.1103/PhysRevE.51.4626.

[5] Mike P Allen and Dominic J Tildesley. *Computer simulation of liquids*. Oxford university press, 1989.

[6] Jean-Pierre Hansen and Ian R McDonald. *Theory of simple liquids*. Elsevier, 1990.

[7] Jos M Thijssen. Computational physics. 2007.

[8] Donald Allan McQuarrie. Statistical thermodynamics. 1973.

[9] Claudio Donati, Silvio Franz, Sharon C Glotzer, and Giorgio Parisi. Theory of non-linear susceptibility and correlation length in glasses and liquids. *Journal of non-crystalline solids*, 307:215–224, 2002.

[10] Pablo G Debenedetti and Frank H Stillinger. Supercooled liquids and the glass transition. *Nature*, 410(6825):259–267, 2001.

[11] Kurt Binder and Walter Kob. *Glassy materials and disordered solids: An introduction to their statistical mechanics*. World Scientific, 2011.

[12] Walter Kob and Jean-Louis Barrat. Aging effects in a lennard-jones glass. *Physical review letters*, 78(24):4581, 1997.

[13] A Rahman. Correlations in the motion of atoms in liquid argon. *Physical Review*, 136(2A):A405, 1964.

[14] William C. Swope, Hans C. Andersen, Peter H. Berens, and Kent R. Wilson. A computer simulation method for the calculation of equilibrium constants for the formation of physical clusters of molecules: Application to small water clusters. *The Journal of Chemical Physics*, 76(1):637–649, 1982. doi: 10.1063/1.442716. URL http://dx.doi.org/10.1063/1.442716.

[15] RK Pathria and Paul D Beale. *Statistical Mechanics,Chapter-16:Computer Simulations*. Elsevier, 2011.

[16] Hans C Andersen. Molecular dynamics simulations at constant pressure and/or temperature. *The Journal of chemical physics*, 72(4):2384–2393, 1980.

[17] Loup Verlet. Computer "experiments" on classical fluids. i. thermodynamical properties of lennard-jones molecules. *Phys. Rev.*, 159:98–103, Jul 1967. doi: 10.1103/PhysRev.159.98. URL https://link.aps.org/doi/10.1103/PhysRev.159.98.

[18] Venkataraman Balakrishnan. *Elements of nonequilibrium statistical mechanics*. Ane Books, 2008.

[19] Pranab Jyoti Bhuyan, Rituparno Mandal, Pinaki Chaudhuri, Abhishek Dhar, and Chandan Dasgupta. Thermal conductivity of glass-forming liquids. *arXiv preprint arXiv:1703.04494*, 2017.

[20] Walter Kob and Hans C. Andersen. Scaling behavior in the β-relaxation regime of a supercooled lennard-jones mixture. *Phys. Rev. Lett.*, 73:1376–1379, Sep 1994. doi: 10.1103/PhysRevLett.73.1376. URL https://link.aps.org/doi/10.1103/PhysRevLett.73.1376.

[21] Smarajit Karmakar, Chandan Dasgupta, and Srikanth Sastry. Growing length and time scales in glass-forming liquids. *Proceedings of the National Academy of Sciences*, 106(10):3675–3679, 2009.

[22] W Gotze and L Sjogren. Relaxation processes in supercooled liquids. *Reports on progress in Physics*, 55(3):241, 1992.